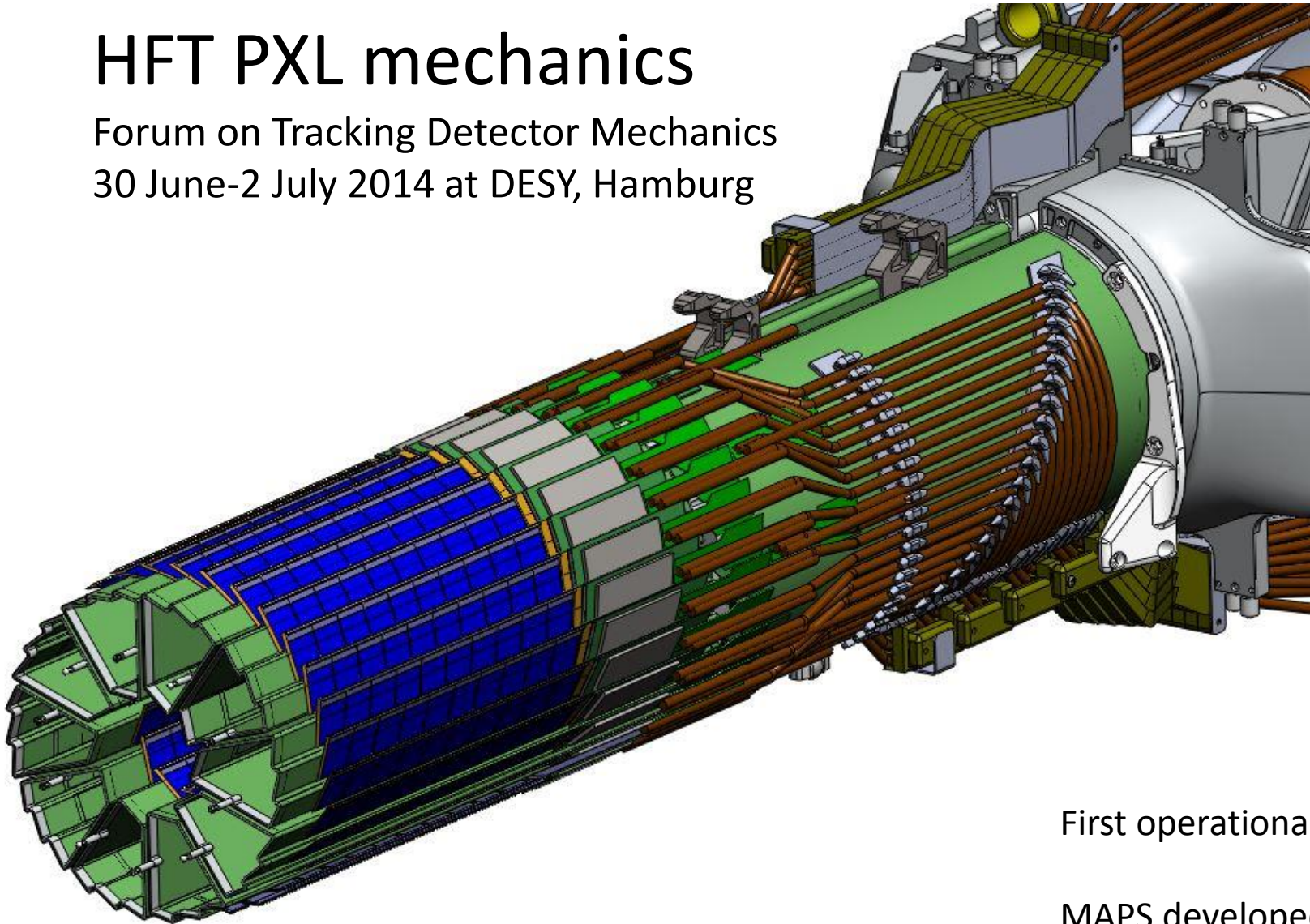


HFT PXL mechanics

Forum on Tracking Detector Mechanics
30 June-2 July 2014 at DESY, Hamburg



LBL
Howard Wieman, Eric Anderssen,
Hao Qui, Leo Greiner, Joe Silber

IPHC-Strasbourg
Michal Szelezniak

First operational vertex detector based on MAPS

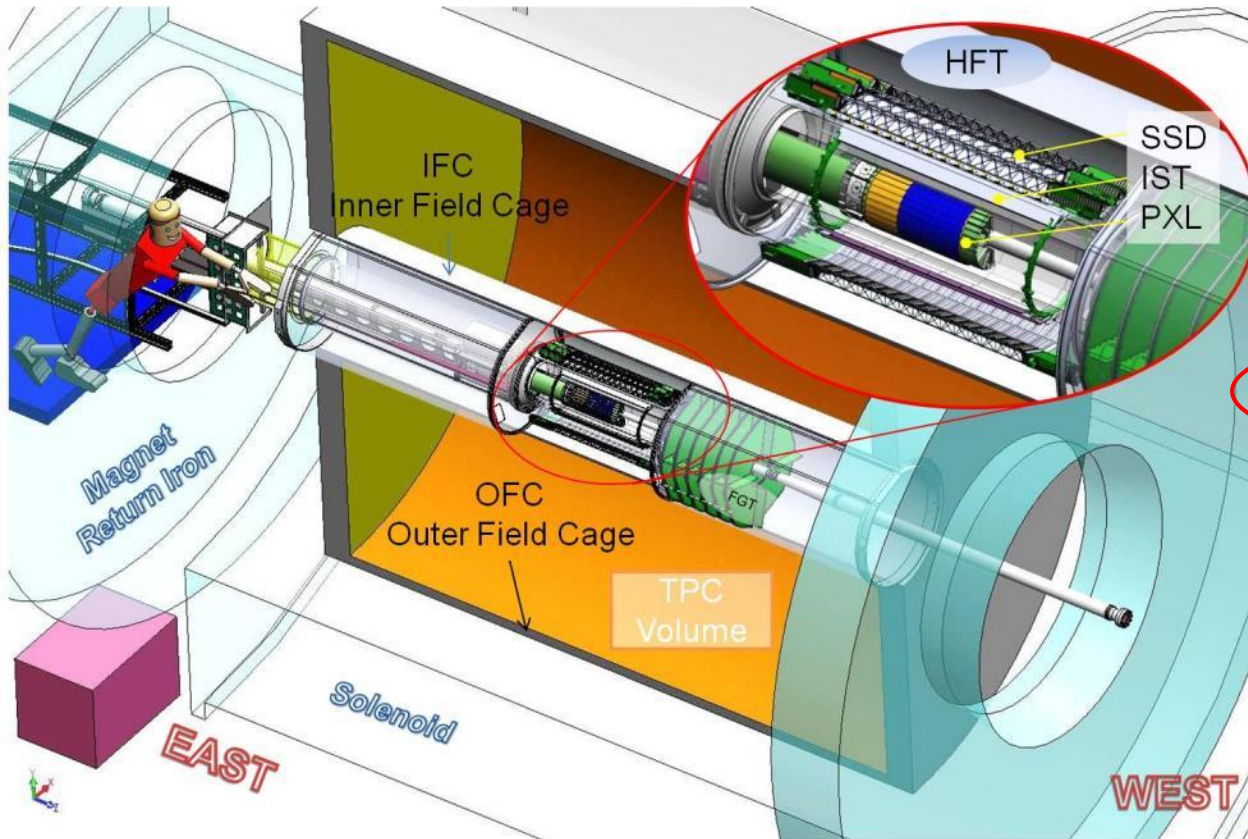
MAPS developed by PICSEL group of IPHC-Strasbourg
(Marc Winter et al.)

Outline

- Introduction to PXL detector in STAR with brief design description.
- The challenge of high resolution and low radiation length
- Mechanical work addressing:
 - Stability against thermal deformation
 - Air cooling
 - Stability against air flow induced vibration and deformation
 - Stability against external support vibration
 - Spatial mapping of the pixel locations
 - Rapid installation and replacement

i.e. how to avoid compromising high resolution potential of MAPS chips

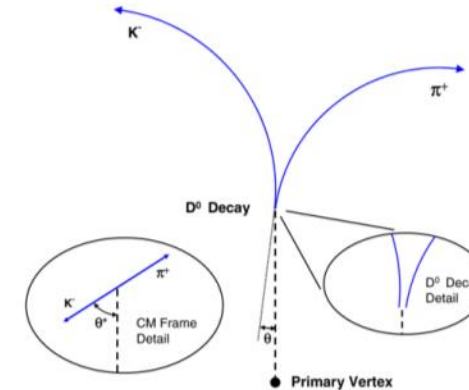
HFT PXL in STAR Inner Detector Upgrades



TPC – Time Projection Chamber
(main tracking detector in STAR)

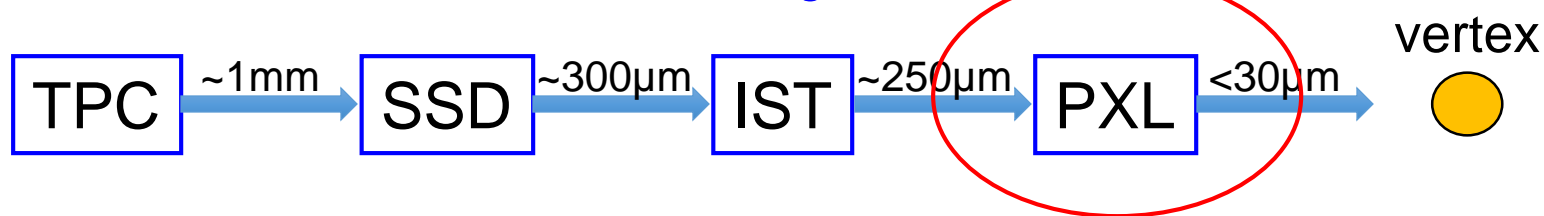
HFT – Heavy Flavor Tracker

- SSD – Silicon Strip Detector
 - $r = 22 \text{ cm}$
- IST – Inner Silicon Tracker
 - $r = 14 \text{ cm}$
- PXL – Pixel Detector
 - $r = 2.8, 8 \text{ cm}$

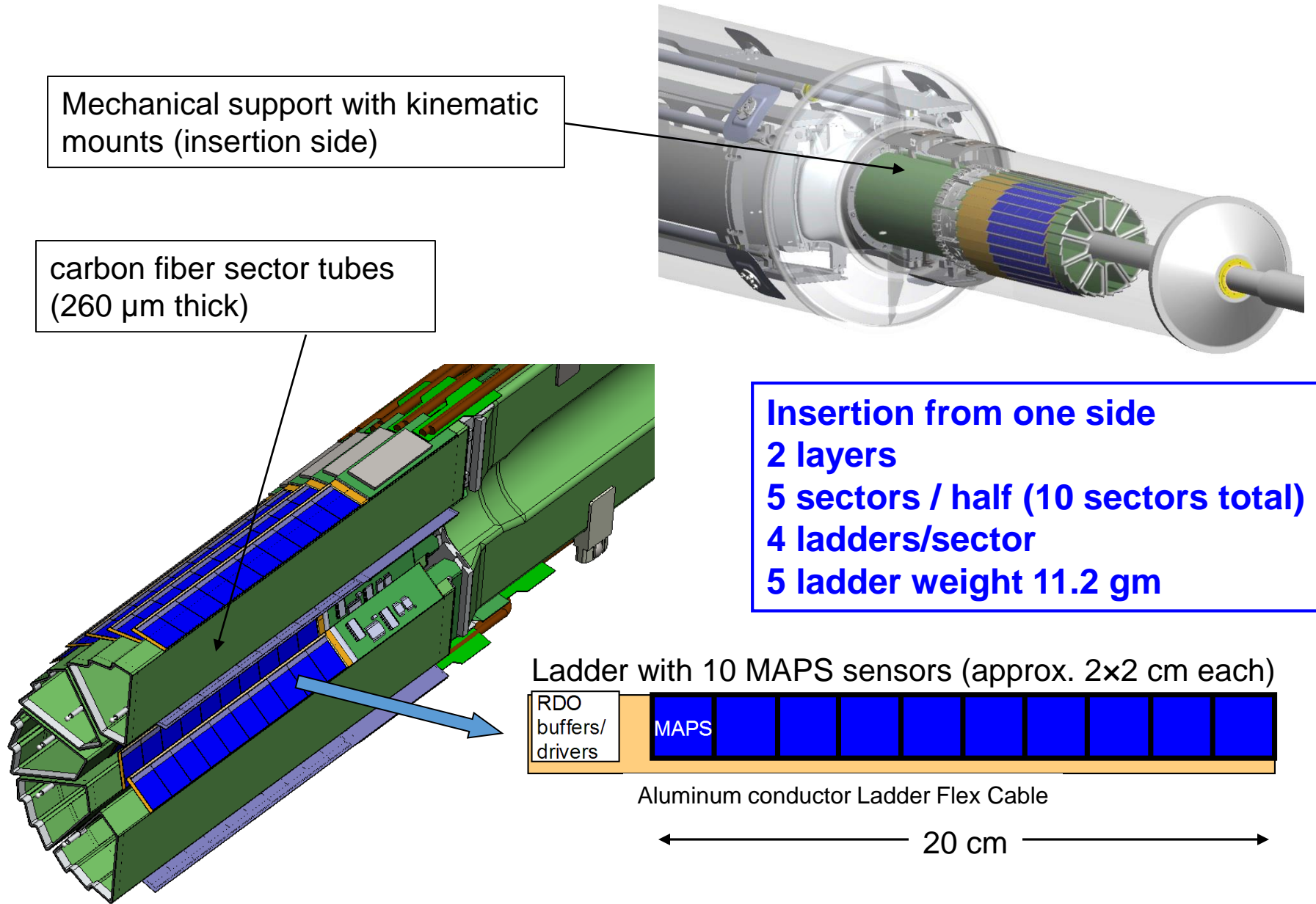


Direct topological reconstruction of Charm

We track inward from the TPC with graded resolution:



PXL Detector Design



PXL Detector Design Characteristics



DCA Pointing resolution	(12* \oplus 24 GeV/p-c) μm
Layers	Layer 1 at 2.8 cm radius Layer 2 at 8 cm radius
Pixel size	20.7 μm X 20.7 μm
Hit resolution	3.7 μm (6 μm geometric)
Position stability	6 μm rms (20 μm envelope)
Radiation length first layer	$X/X_0 = 0.39\%$ (Al conductor cable)
Number of pixels	356 M
Integration time (affects pileup)	185.6 μs
Radiation environment	20 to 90 kRad / year $2 \cdot 10^{11}$ to 10^{12} 1MeV n eq/cm ²
Rapid detector replacement	\sim 1 day

356 M pixels on $\sim 0.16 \text{ m}^2$ of Silicon

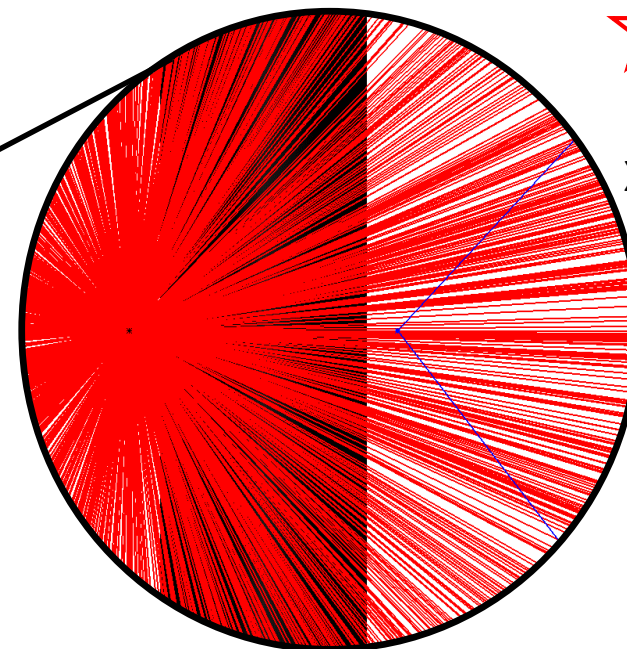
* Simple geometric component, cluster centroid fitting gives factor of ~ 1.7 better.

Au + Au 200 GeV central collision, $\eta \pm 1$
 $dN/d\eta$ 650

The challenge

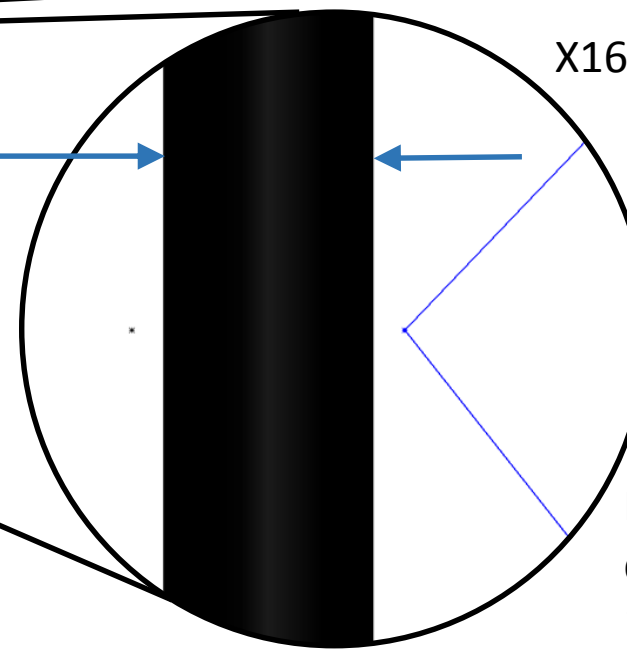


X160



X160

100 μm
human hair
for scale



D meson
decay τ
130 μm

Inner layer HFT PXL detector

The advantage of improved spatial resolution and reduced radiation length

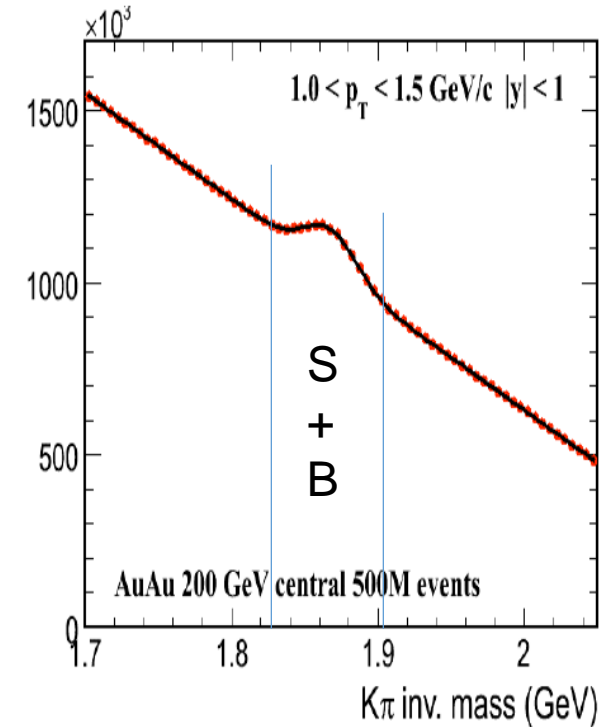
Compare simulated detector performance in number of events required to reach a given significance:

$$\frac{\text{signal}}{\sqrt{\text{signal} + \text{background}}}$$

Simulation results

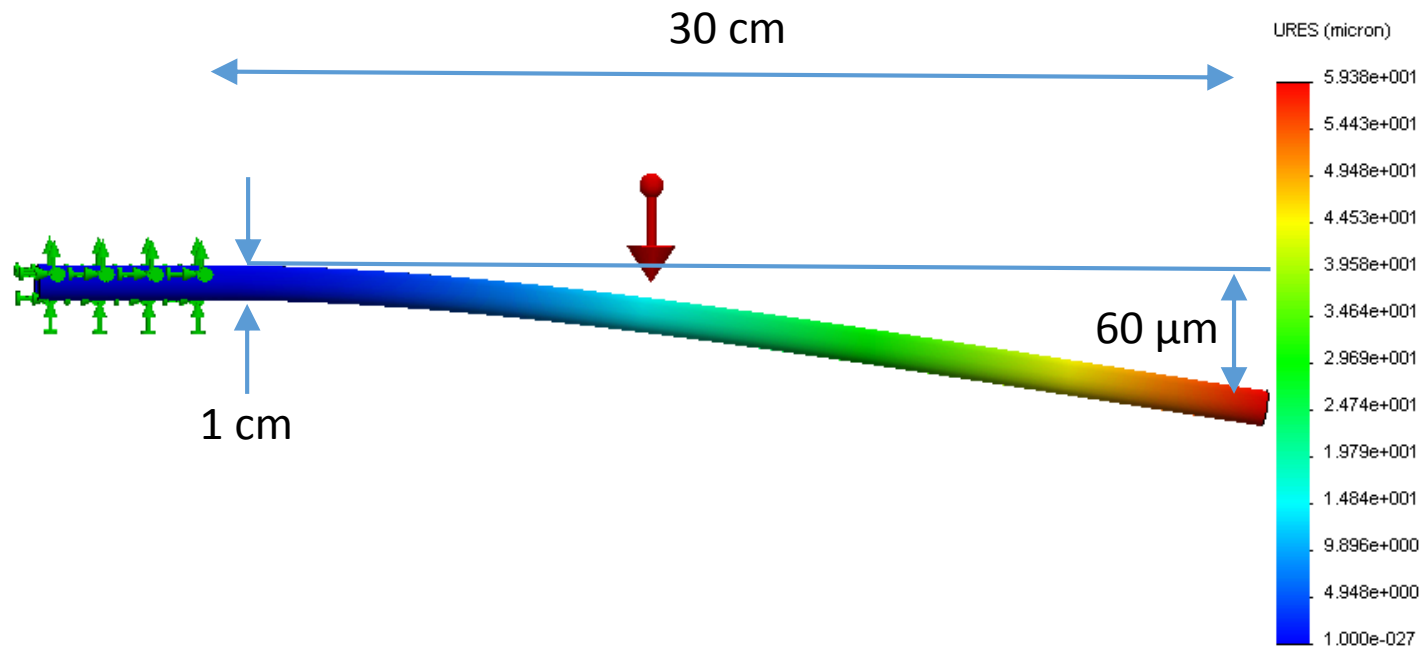
	Pixel size	radiation length	0.5 GeV D_0 relative number of events	1.5 GeV D_0 relative number of events
hybrid	50 μm x 450 μm	1.4%	36	200
MAPS	27 μm x 27 μm	0.6%	1	1

parameters used in the simulation, but actual HFT PXL parameters are smaller



Stability and reduced radiation length requirement makes for an interesting mechanical challenge

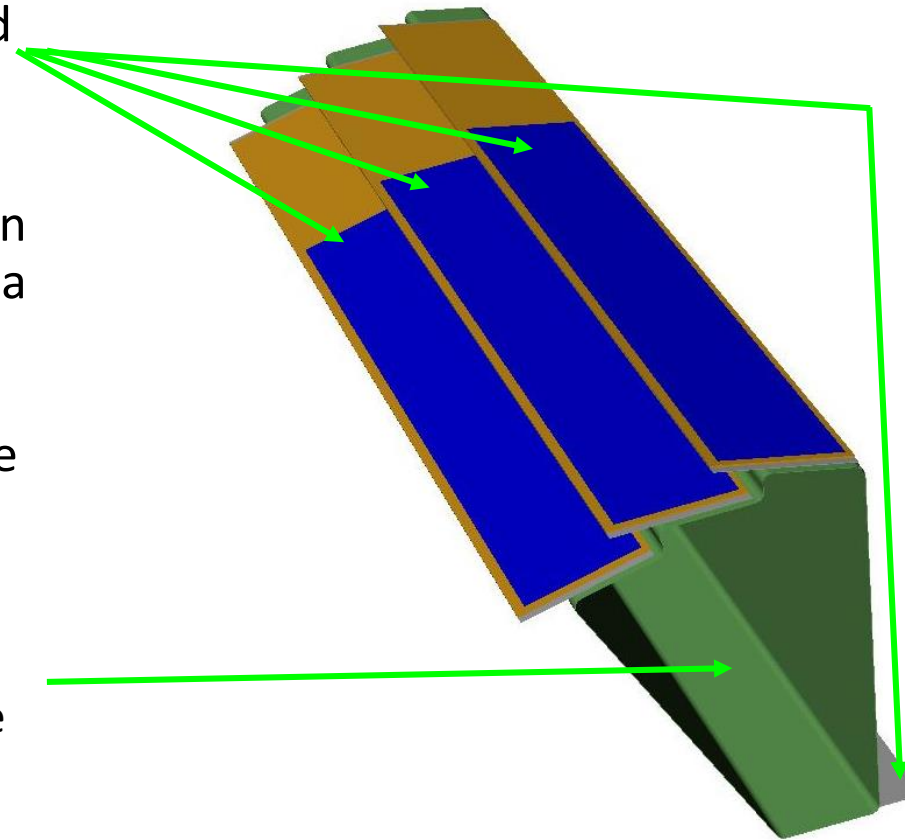
The MAPS pixels are 20 μm square on thinned (50 μm) silicon. The mechanical stability and alignment should not compromise this potential position resolution. And the mass of support structures should not compromise the potential reduced multiple coulomb achieved with thinned silicon.



To give a feeling for what 20 μm means mechanically, consider a 1 cm steel rod projected 30 cm. The sag due to gravity is 60 μm

Controlling thermal induced deformation

- The detector ladders are thinned silicon, on a flex kapton/aluminum cable
- The large CTE difference between carbon composite and kapton is a potential source of thermal induced deformation even with modest 10-15 deg C temperature swings
- Two methods of control
 - ALICE style carbon composite sector support beam with large moment of inertia
 - Soft decoupling adhesive* bonding ladder layers

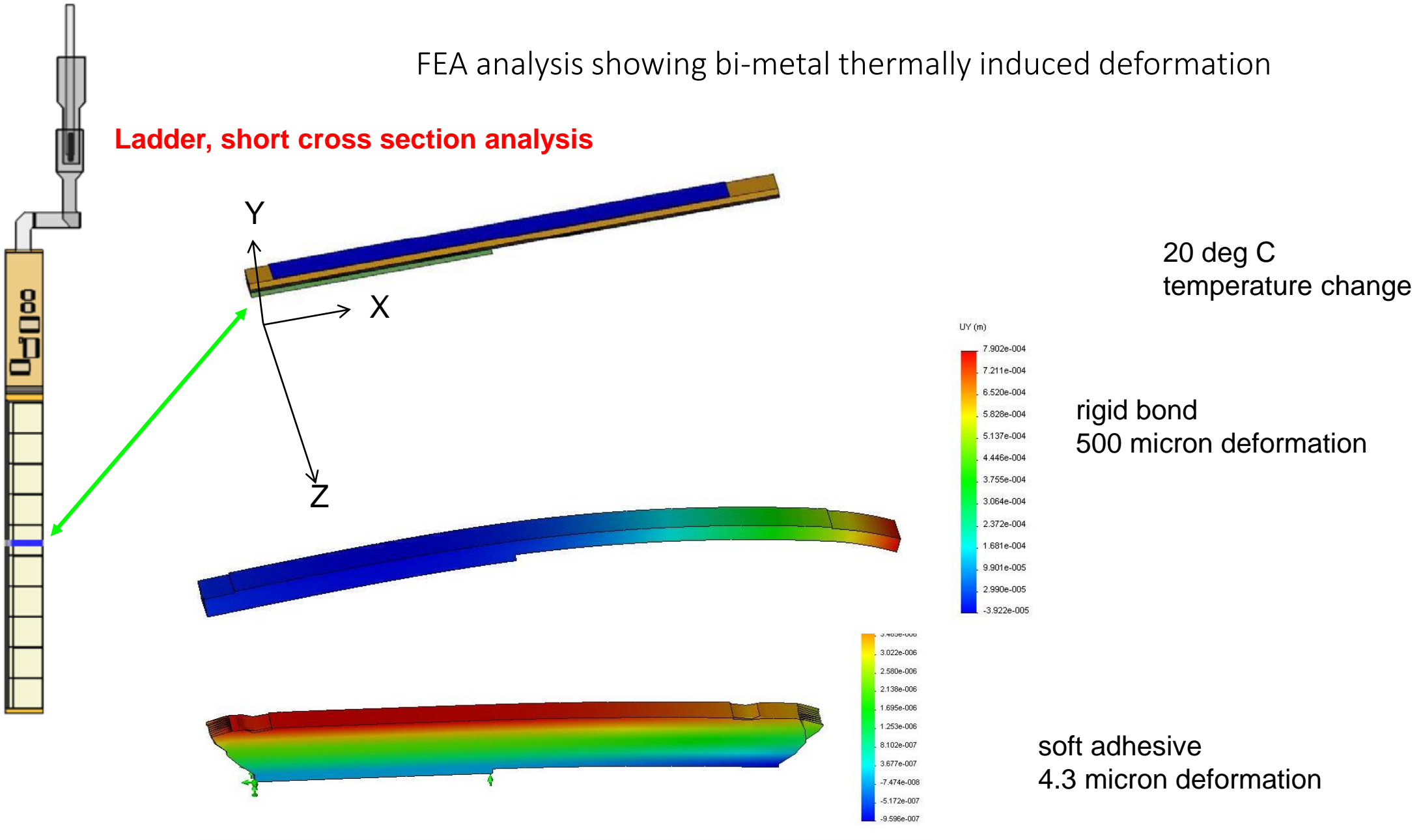


* 3M 467MP 200MP adhesive, acrylic 2 mil sheet, shear modulus 1.5×10^4 Pa (2 psi)

Considered other ladder and sector design structures, but this approach offered good stiffness to mass as well as good air cooling

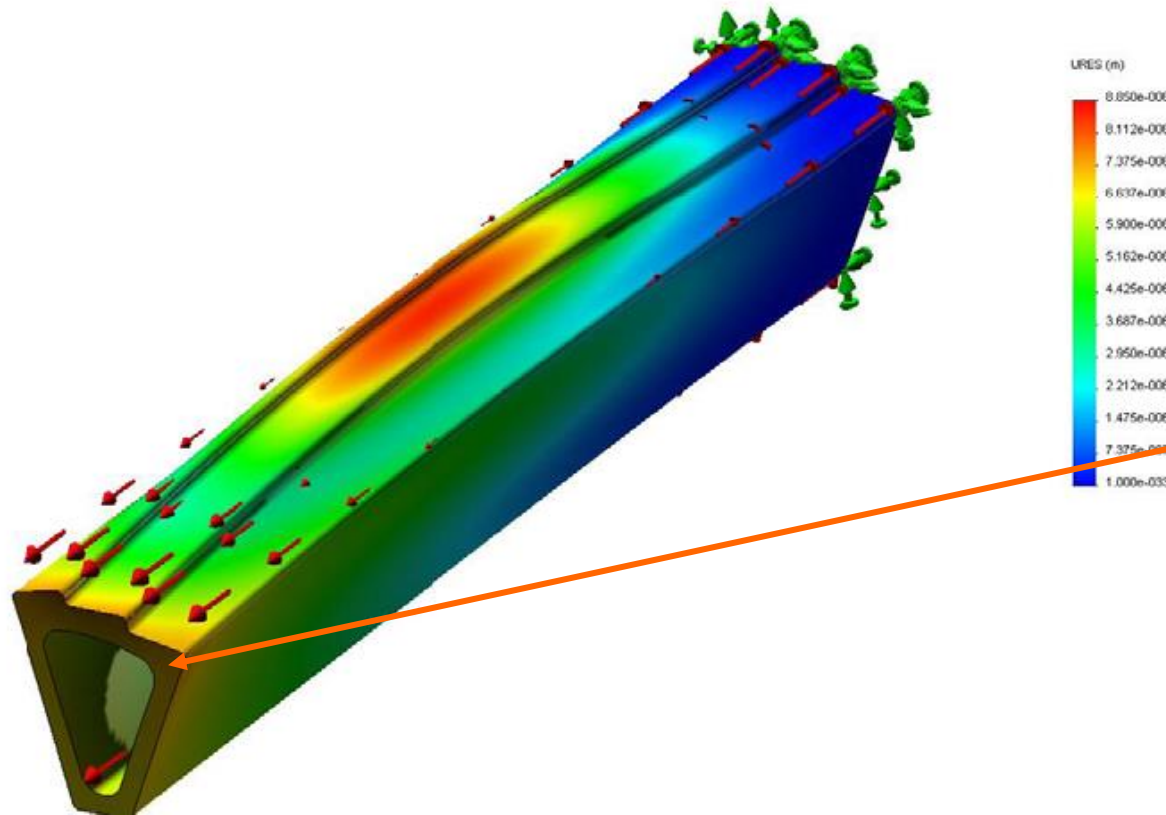
FEA analysis showing bi-metal thermally induced deformation

Ladder, short cross section analysis



Timoshenko, S. Analysis of bi-metal thermostats. J. Opt. Soc.Am. 1925, 11, 233-255,
if you don't want to take the easy way out with FEA

FEA analysis of thermally induced deformation of sector beam

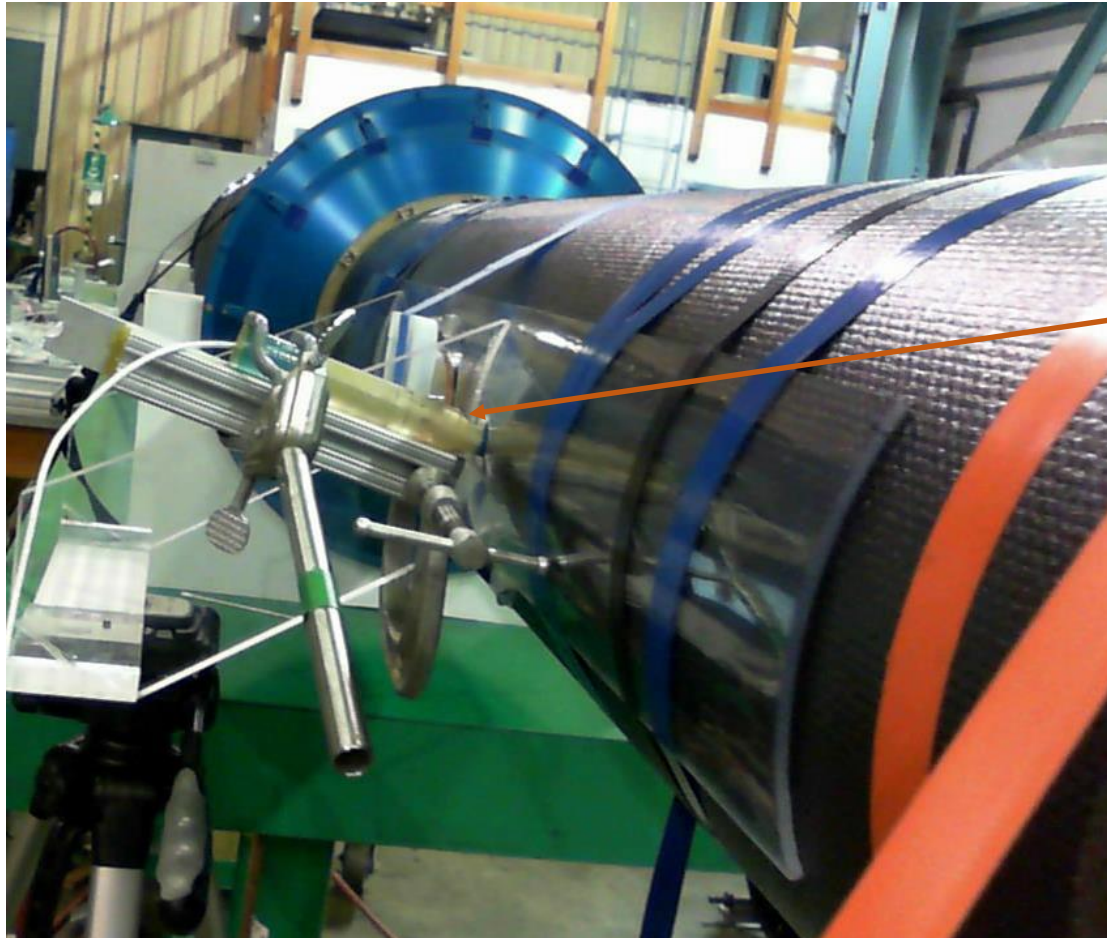


- FEA shell elements
- Shear force load from ladders
- 20 deg temperature rise
- Soft adhesive coupling
- 200 micron carbon composite beam
- end cap reinforcement
- **Maximum deformation 9 microns** (30 microns if no end cap)

Final measurement of thermal deformation with completed system.

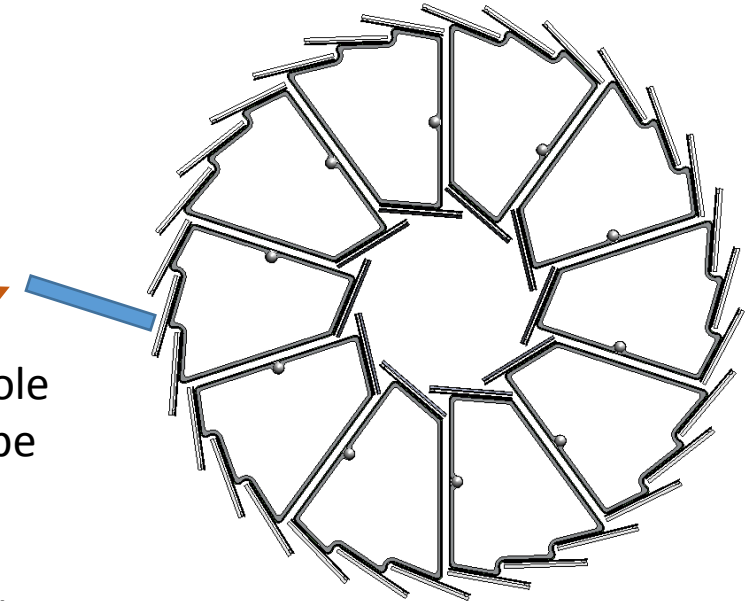
probe:
Lion Precision
Model: C1-A
500 μm range
2.0 nm RMS resolution
<http://www.lionprecision.com/>

Same setup used to measure vibration and air pressure displacement, more on this to follow



capacitive probe inserted through hole in Pixel Support Tube (PST) at $z \sim 12$ cm, this is on sector beam just past active ladder

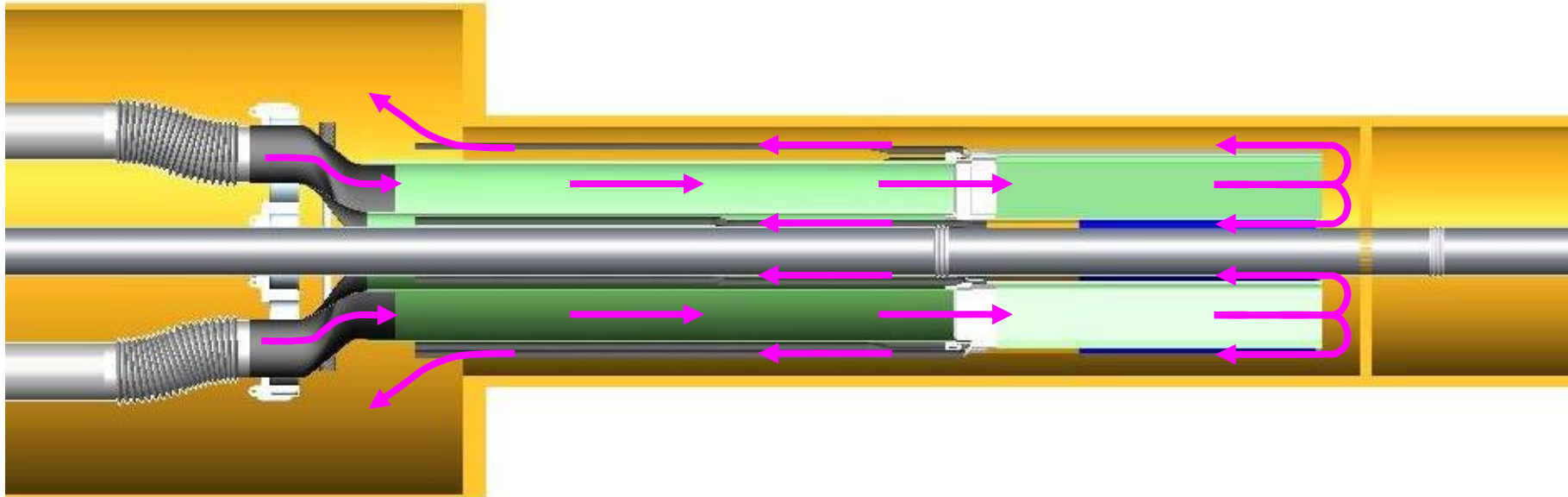
North half sectors populated with operating ladders. South half populated with empty sector tubes. System operated with full cooling air



Position change between sector power off and on
ladder moves $3 \mu\text{m}$ to $8 \mu\text{m}$ toward center when powered ($\sim 10^\circ\text{C}$ change)

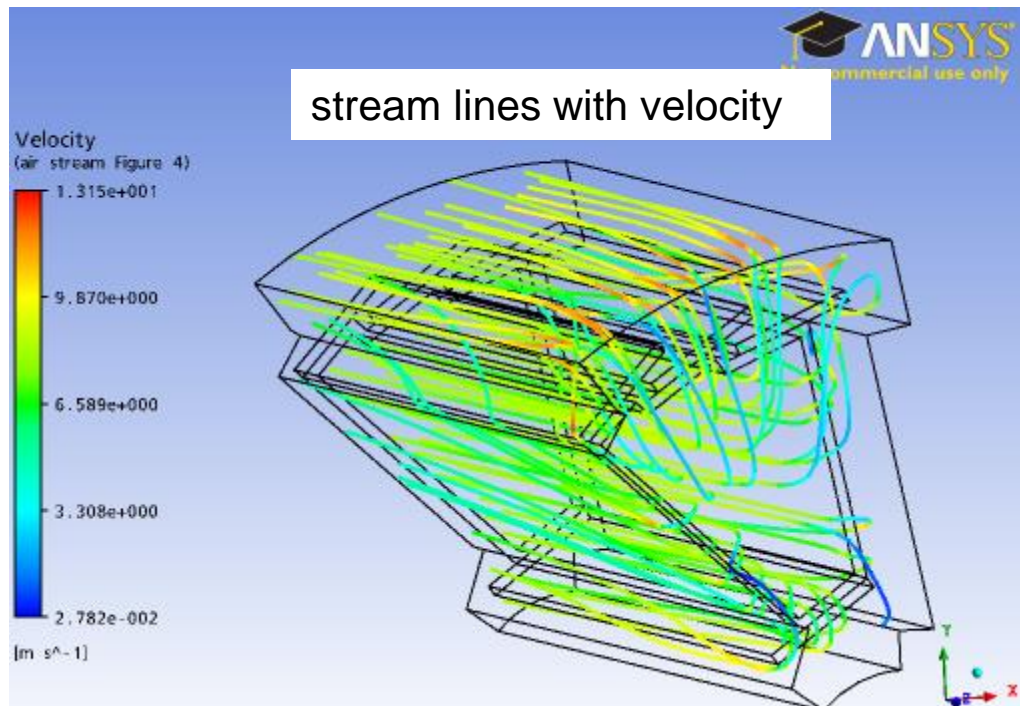
Air cooling of silicon detectors - CFD analysis

- Silicon power: 100 mW/cm^2 (~ power of sunlight)
- 240 W total Si + drivers

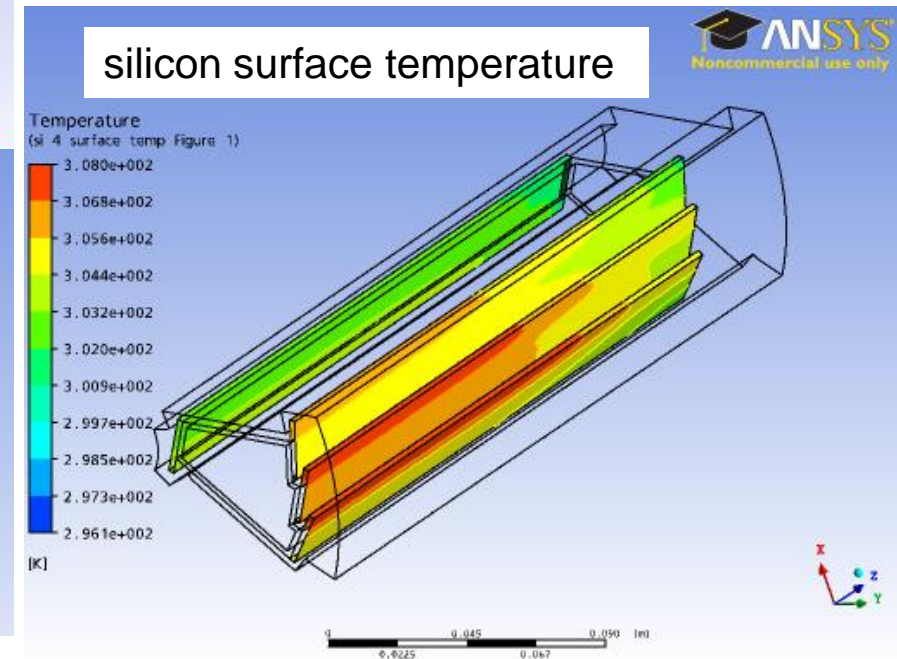
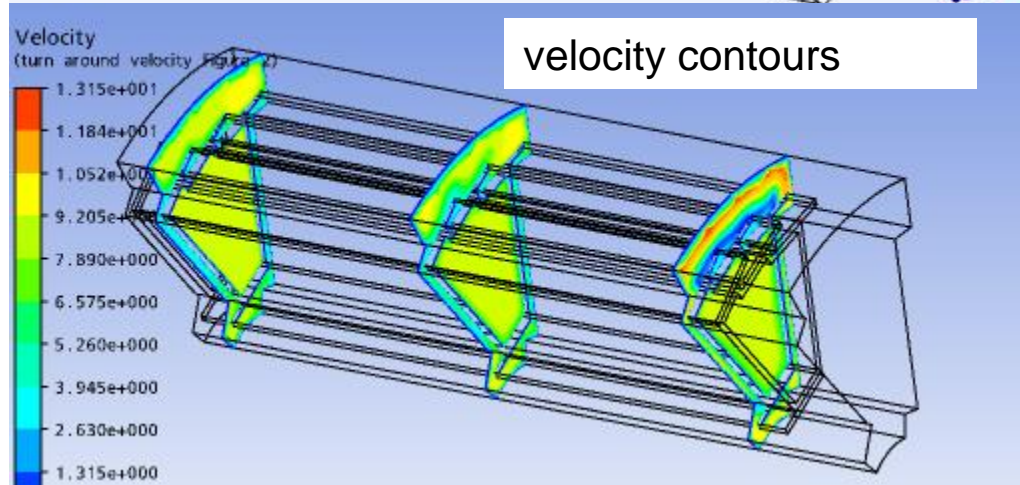


air flow path – flows along both inside and outside surface of the sector

Air cooling – Computational Fluid Dynamics (CFD) analysis

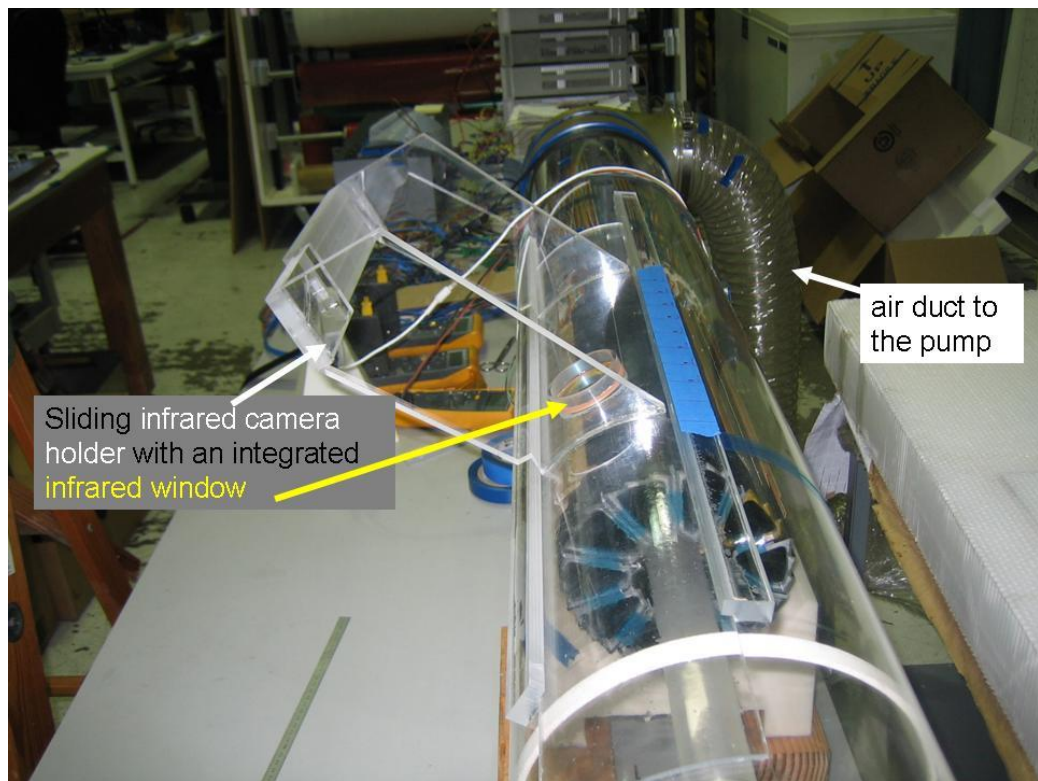


- air flow velocity 9-10 m/s
- maximum temperature rise above ambient: 12 deg C
- sector beam surface – important component to cooling
- dynamic pressure force 1.7 times gravity

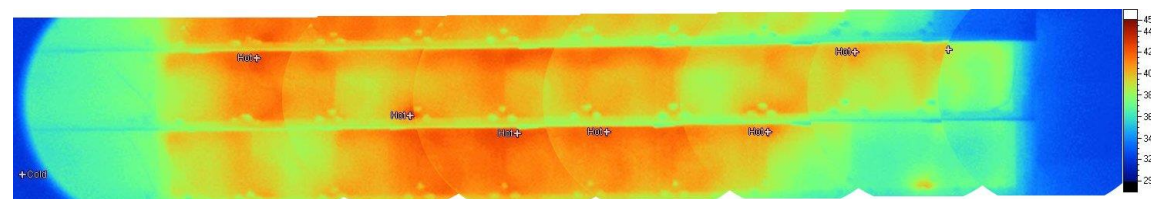


Full scale mockup to verify cooling capability

- Platinum on thinned silicon to simulate detector chip heat load
- Additional heaters to reproduce driver heat sources
- Input and output thermocouple monitoring of air temperature
- Thermistors distributed on mockup pixel ladders
- IR camera to measure surface temperatures
- Air blower with static head of 9 inches of water
- air velocities measured with a hot wire velocity sensor



In these tests we failed to get good total mass flow measurements which complicated specifying the final cooling blower system.

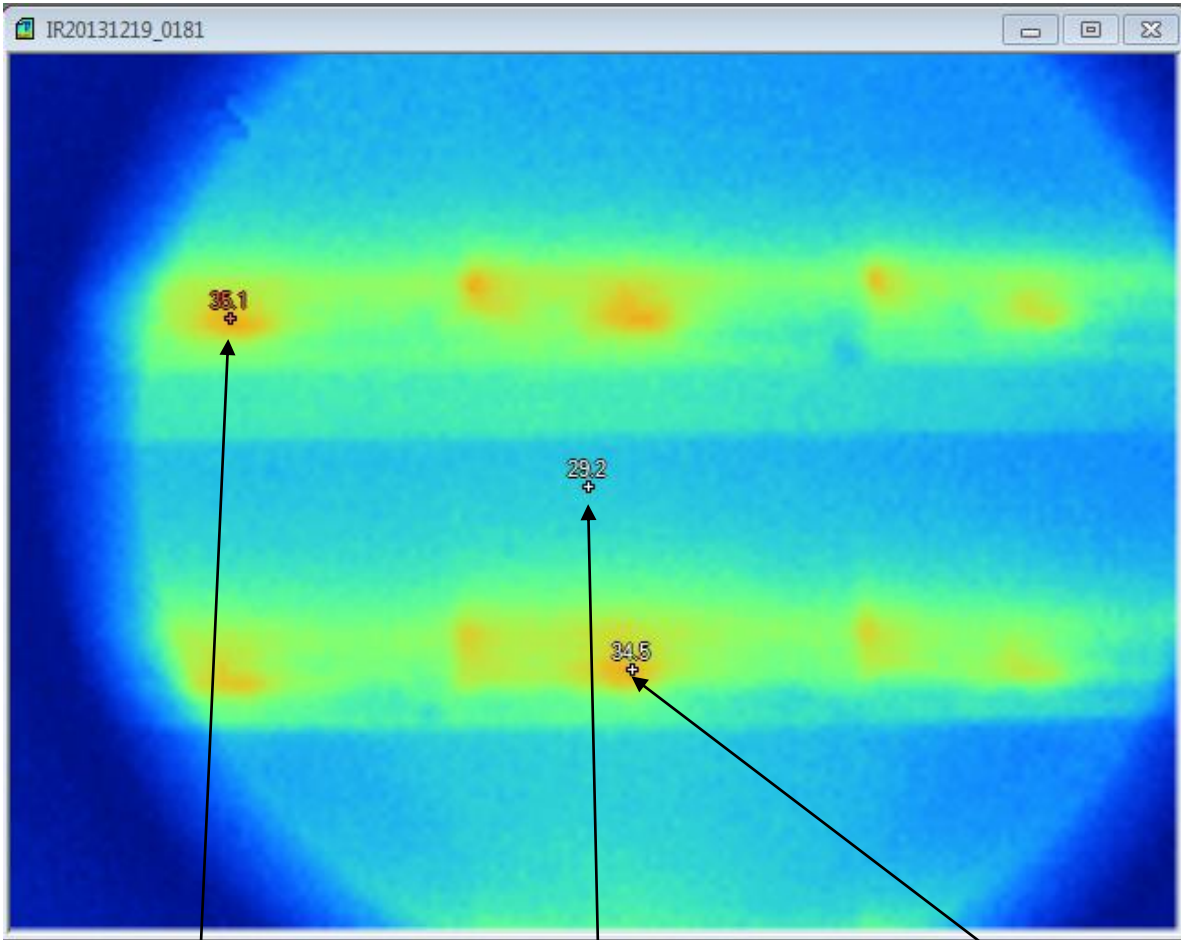


Thermal image of sector-1 at 290 W dissipated in the detector and at the air flow speed of 12.2 m/s. The image was stitched from 8 individual images of small subsections. Ambient air temperature 31 °C

Result: $\Delta T = 11 \text{ }^\circ\text{C}$ with 10.4 m/s air velocity, verifying CFD estimate

test of operating PXL system with full power and cooling flow

Ladders viewed through IR window installed in the Pixel Support Tube



hottest point on the chip, middle of the digital section.

center of the middle chip (active region)

center of the digital section of the middle chip

Air Innovations
Cooling air supply
.14 m³/s
at 2200 Pascal
temperature regulated to 23±1 °C

PXL detector assembly

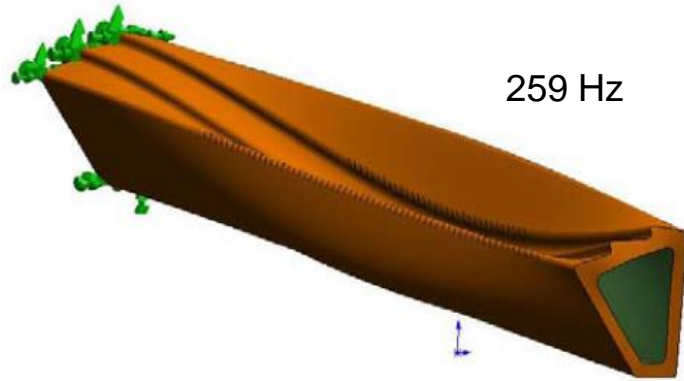


12 °C
MAX deviation
from ambient

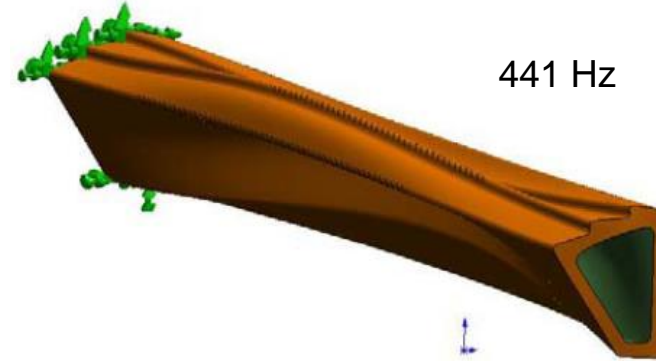
Static displacement and vibration induced by cooling air flow

- Sector vibration modes were examined with FEA
- Prototype sector vibrations measured with airflow tests. This was determined to be less time consuming than setting up transient CFD calculations.
- Measurement of completed detector

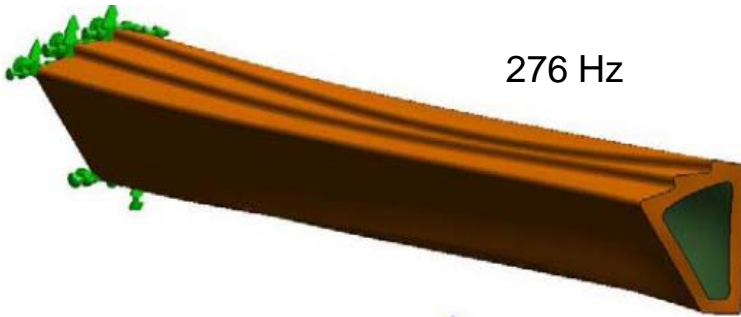
vibration modes



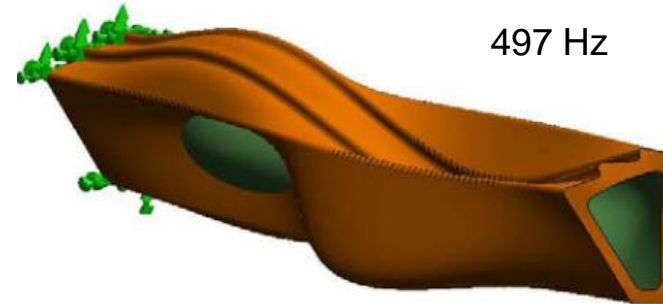
259 Hz



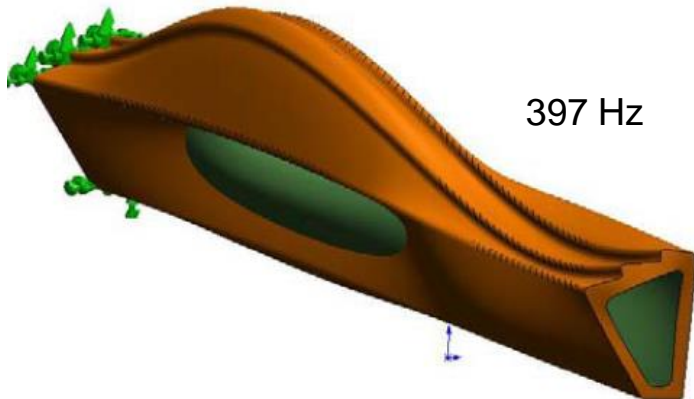
441 Hz



276 Hz



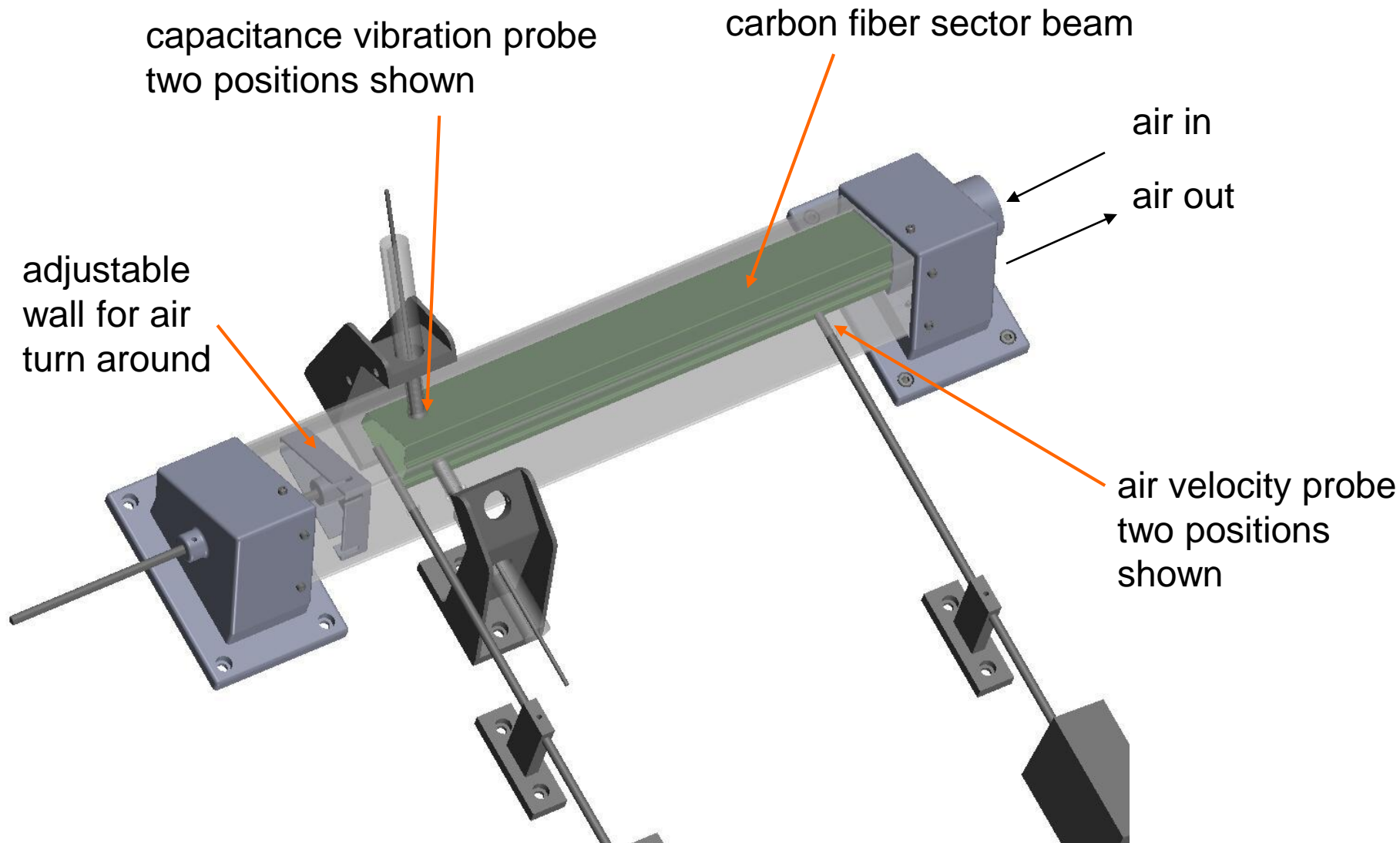
497 Hz



397 Hz

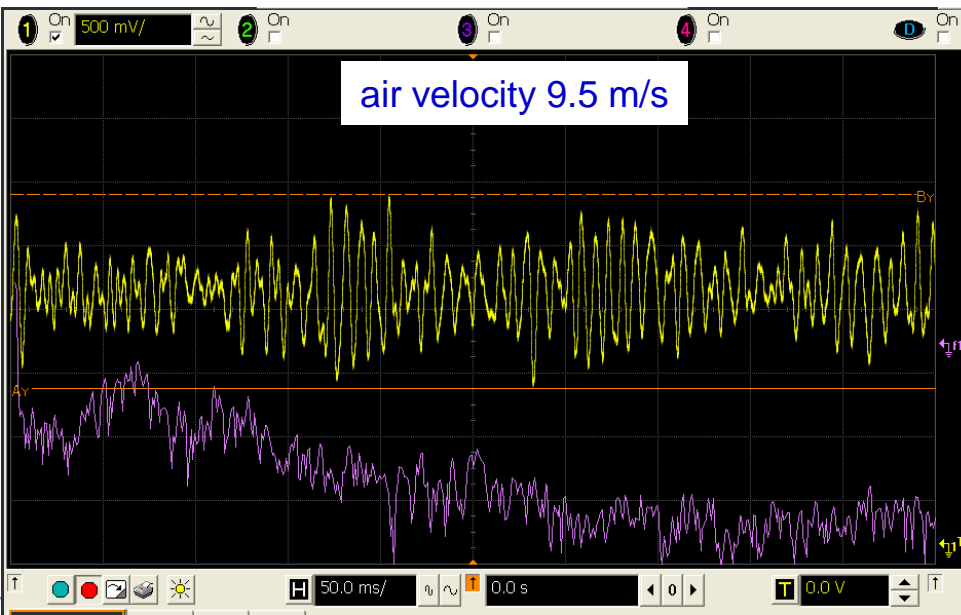
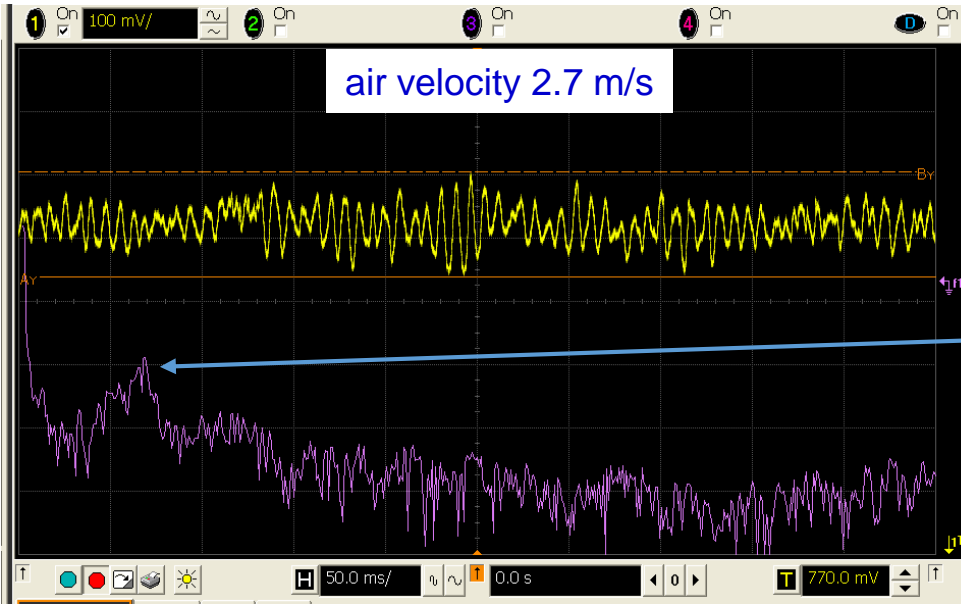
- Lots of complicated modes close in frequency

wind tunnel setup to test vibration and displacement



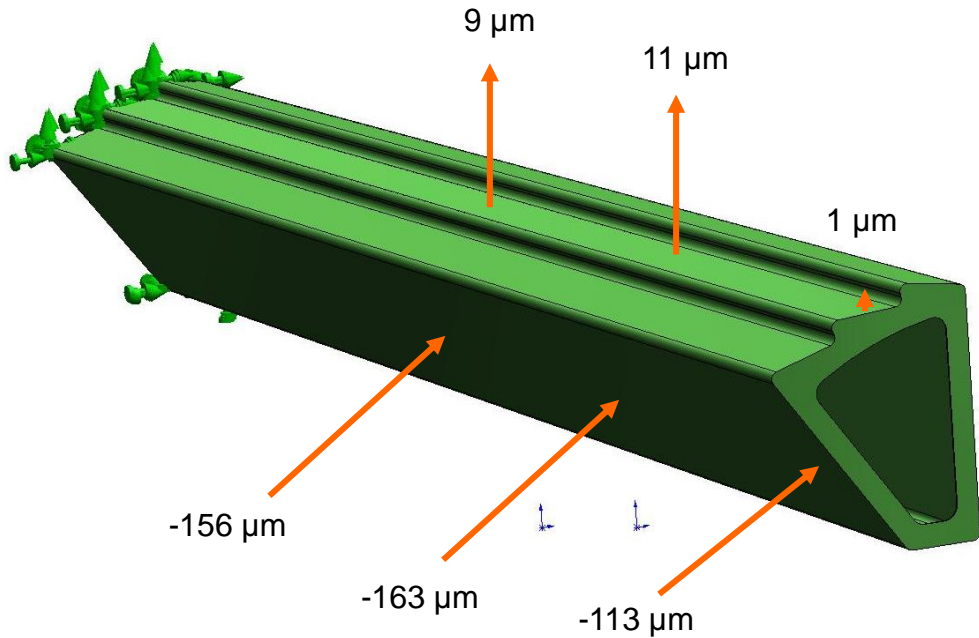
capacitive probe vibration measurements

proto type sector
wind tunnel test



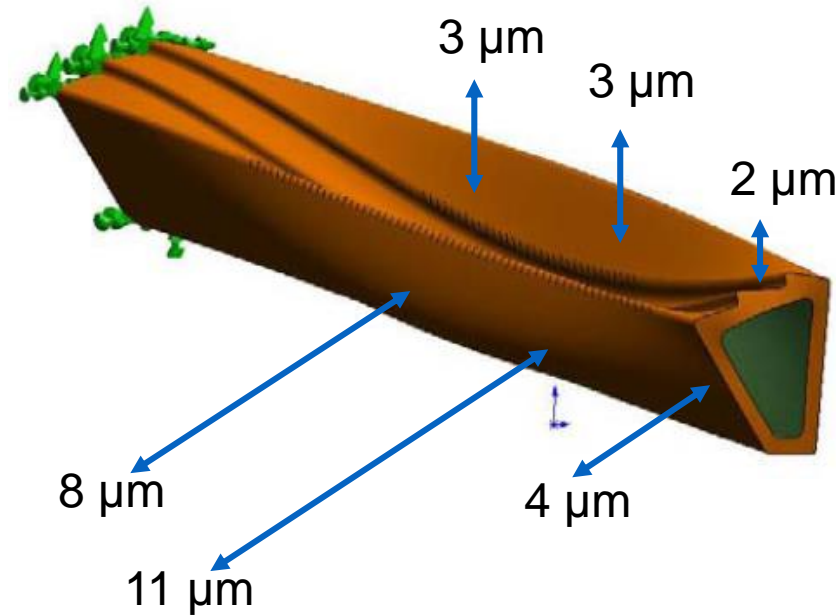
effect of 9 m/s air flow

proto type sector
wind tunnel test



static deformation

shapes of simulated 1st
vibrational mode shown for
qualitative comparison only



vibration (RMS)

Radial sector motion measured with capacitive probe inserted through hole in PST

capacitive probe
measurement of
completed PXL detector

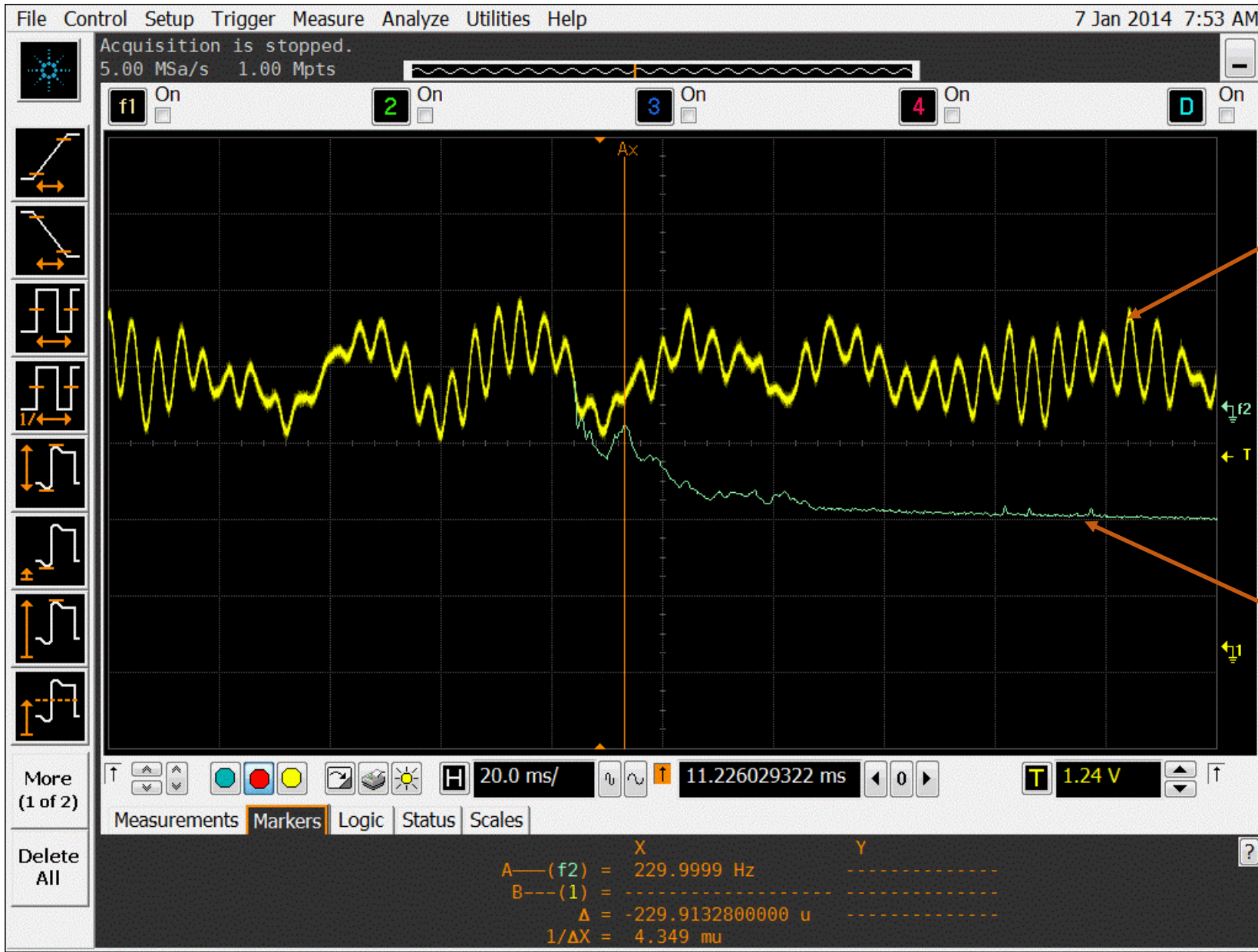


North half sectors populated with operating ladders. South half populated with empty sector tubes. System operated with full cooling air

Typical screen shot at full air flow

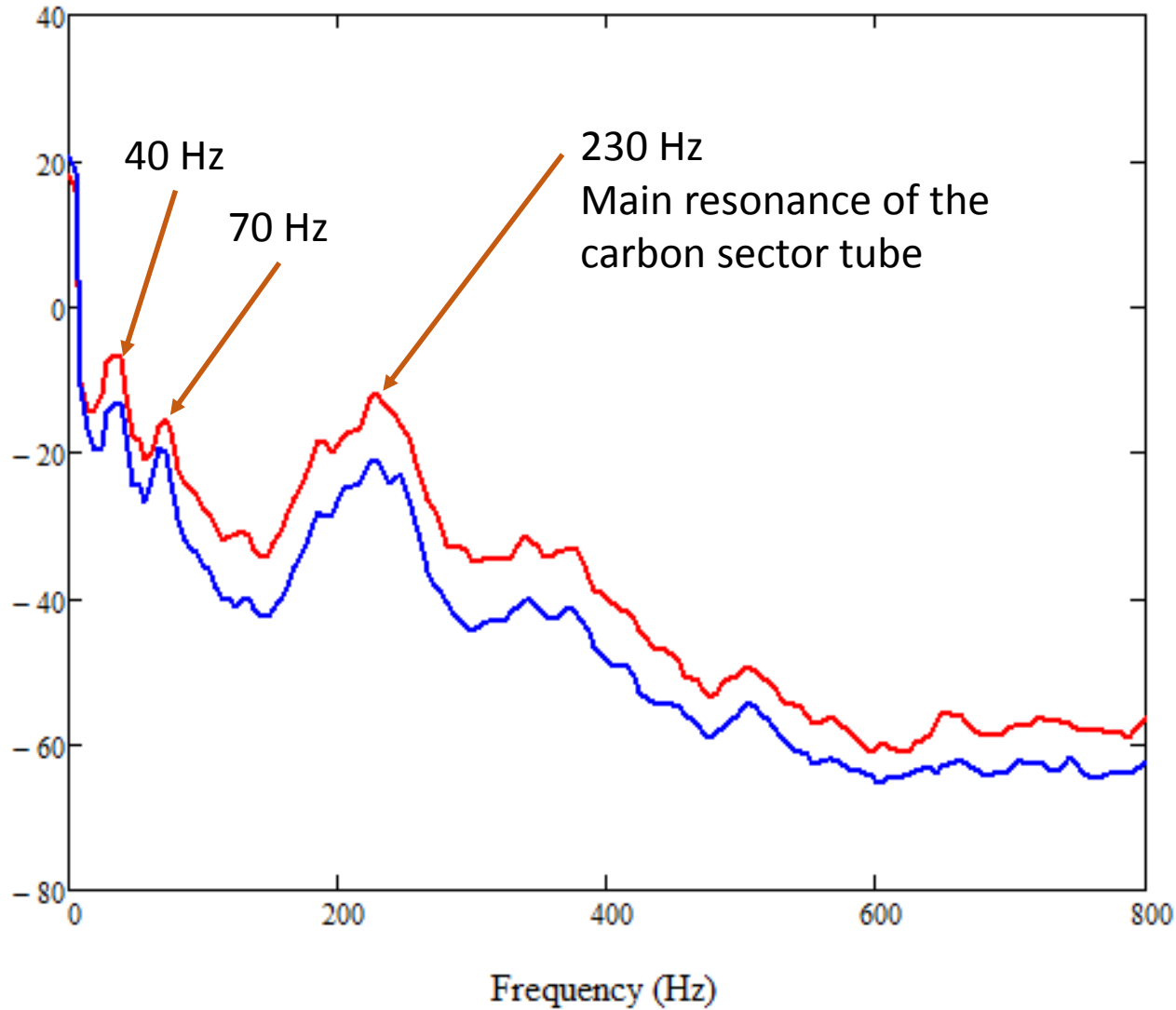


capacitive probe
measurement of
completed PXL detector



Fourier transform of sector vibration

capacitive probe
measurement of
completed PXL detector

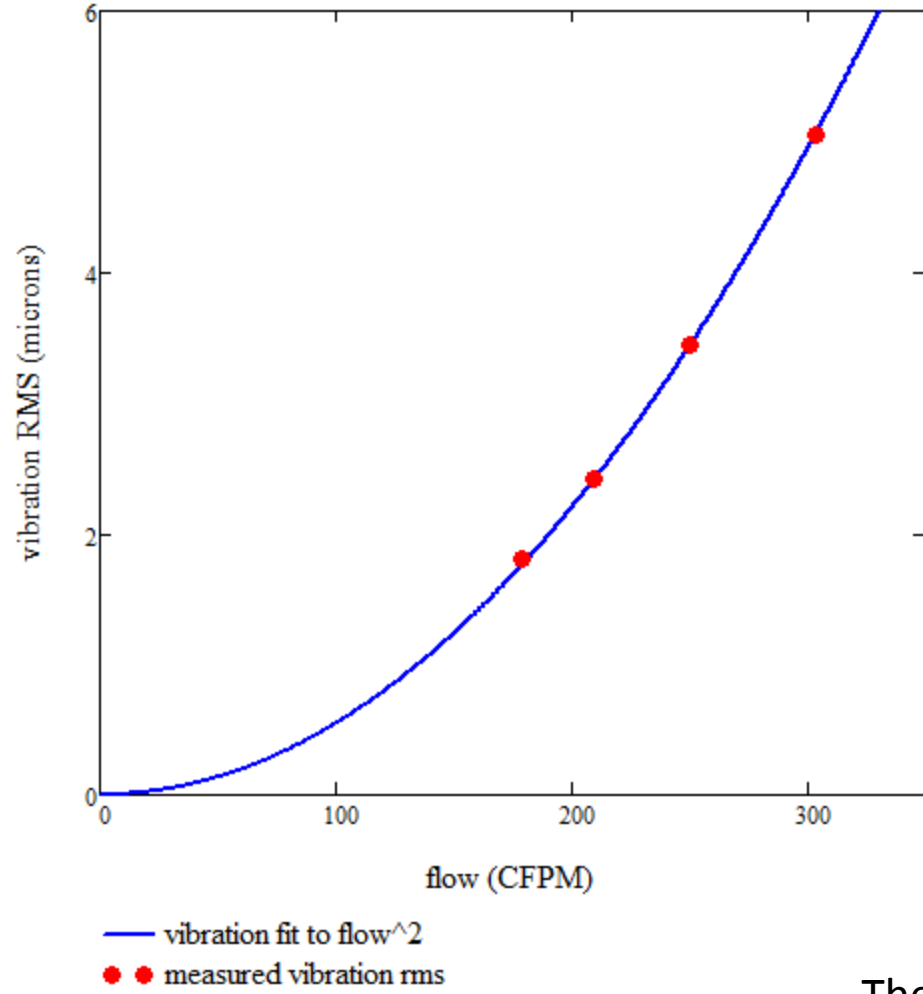


close to 260 Hz from
original FEA simulation

— fit at max flow
— fit at 69% max flow

Measured sector radial vibration as a function cooling air flow for edge ladder

capacitive probe
measurement of
completed PXL detector



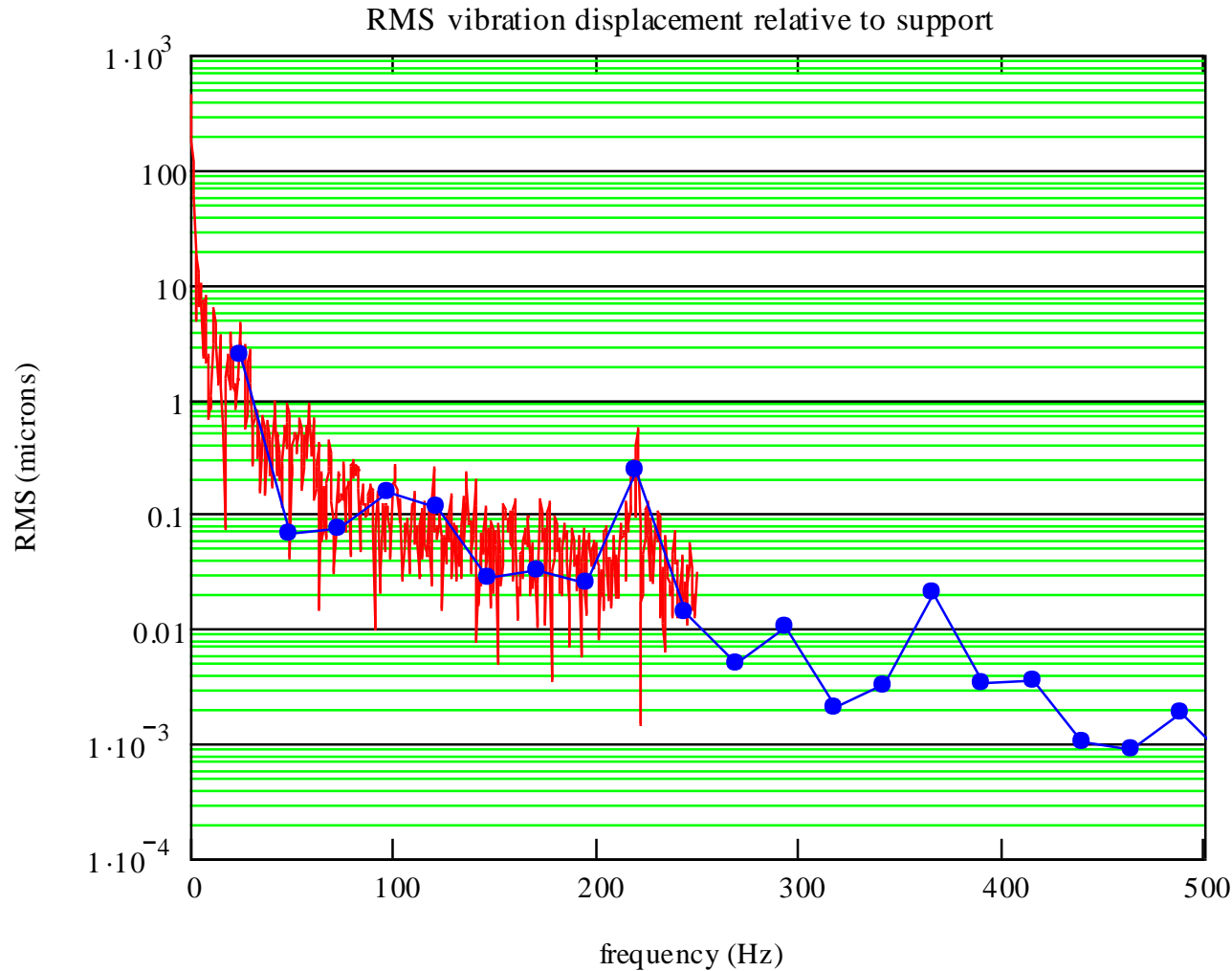
The measured vibration with no air flowing: 35 nm RMS

capacitive probe
measurement of
completed PXL detector

cooling air induced vibration and static displacement

Sector vibration in the radial direction scales as:	flow ²
Sector vibration at full flow:	5 μm RMS
Sector DC displacement scales as:	flow ²
Sector moves in radially at full flow:	25 μm - 30 μm

Vibration from STAR support, accelerometer measurement



Early in the project an accelerometer was mounted on the support point in STAR while STAR was operating with the magnet on to determine if support vibration could affect the PXL pointing resolution.

The vibration magnitude is assessed for a harmonic oscillator driven by the acceleration power spectrum.

- detector vibration from STAR support < 0.1 micron RMS

For this analysis used an earlier ladder prototype. The study was not updated with the final sector design because it was clear that this external vibration effect was not important

Resonance frequency and Q, damping obtained from capacitive probe measure of the ladder vibration as it decayed



If a harmonic oscillator mechanical structure is mounted on a vibrating support the RMS displacement relative to the support is given approximately as:

$$Z_{rms} = \sqrt{\frac{\pi \cdot Q \cdot PSD(\omega)}{2 \cdot \omega^3}} \quad [1]$$

+

where

ω is the radial resonant frequency of the oscillator

PSD(ω) is the acceleration² density at the resonant frequency

and Q is the Q of the oscillator.

References:

- Eq. 11.38 from "Shock & Vibration Handbook, Vol 1. Basic Theory & Measurements", Harris & Crede, 1961 McGraw-Hill, Library of Congress card catalogue number 60-16636

accelerometer:

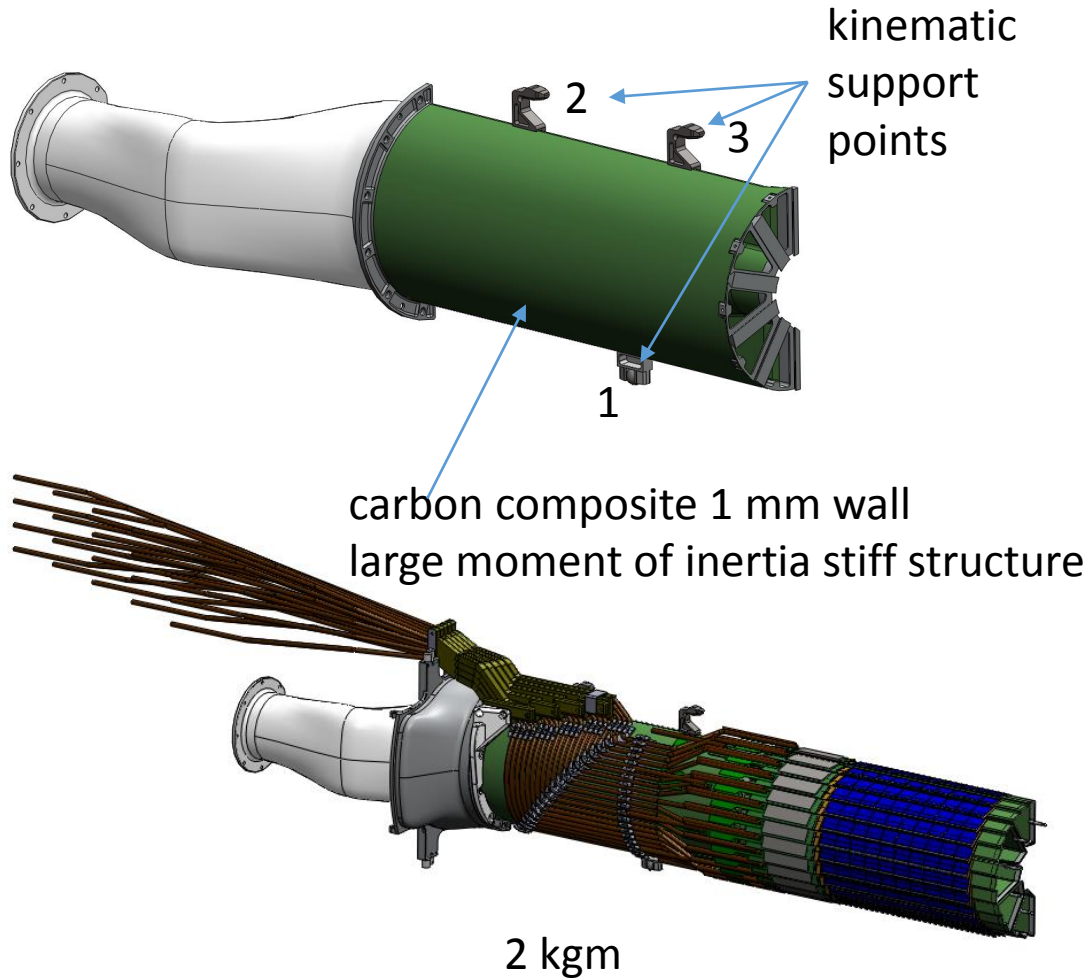
Endevco

Model 86

Seismic accelerometer

<https://www.endevco.com/>

PXL support structure control of external forces



load source	load (kgf)
gravity	2
possible dynamic air pressure 10 m/s	0.5
signal cable stiffness, controlled using very fine twisted pairs, 160 μm wire.	negligible
power cable stiffness, multi conductor 130 μm strands	negligible
flexible air ducting	unknown

Early FEA analysis showed sub micron distortions, but no analysis done with final loads and design details.

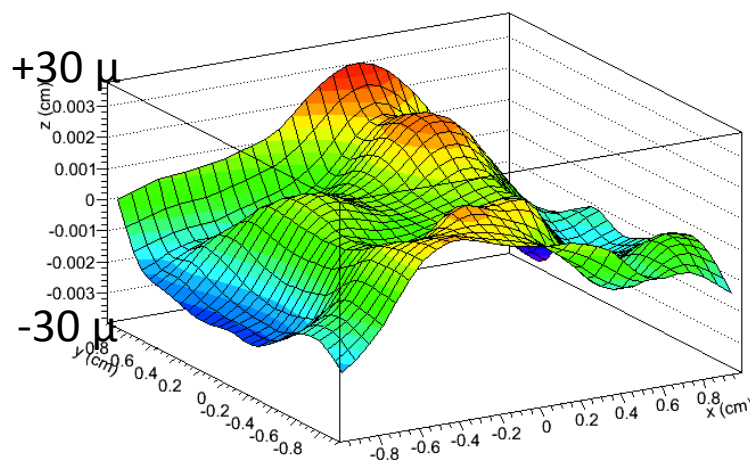
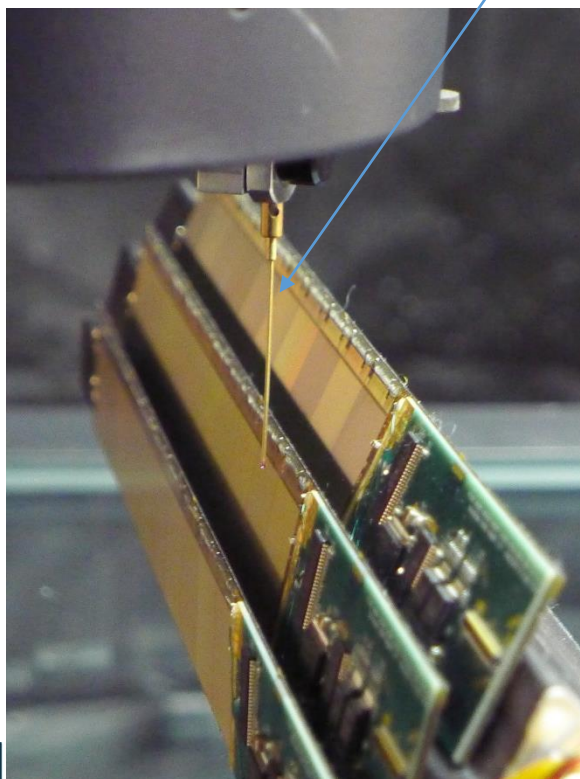
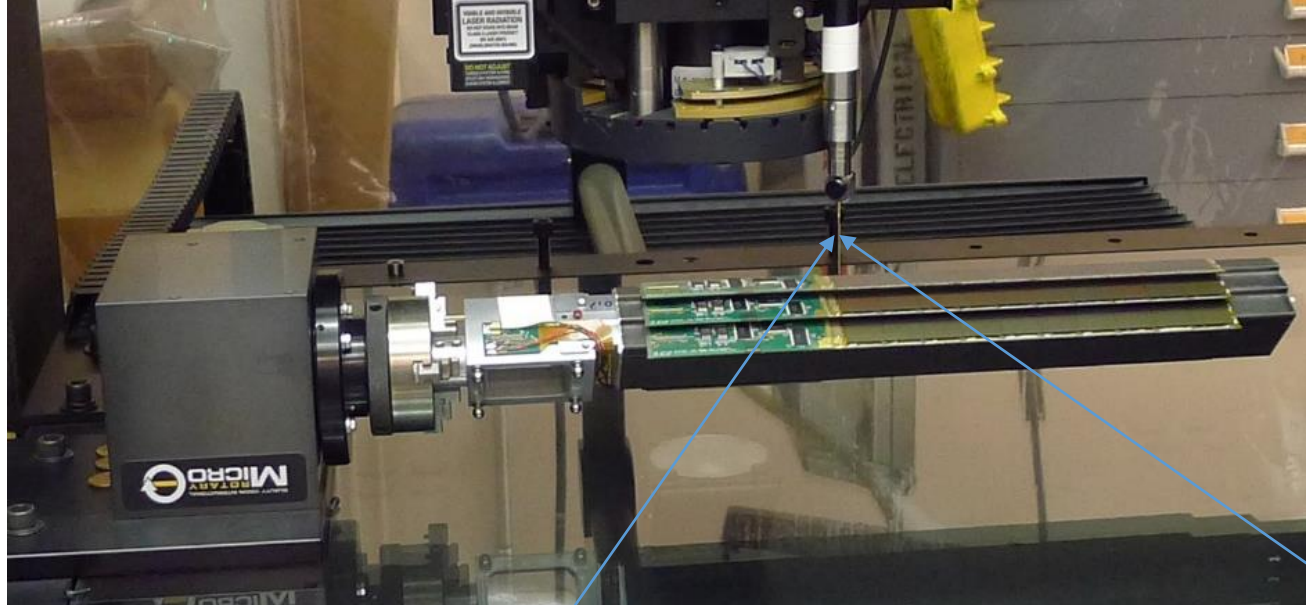
Could not find easy analysis for flexible air ducting to cover reaction to air velocity changes and air frictional forces. Decided to address decoupling after construction if a problem was found, dogged a bullet on this one.

Spatial mapping of the pixels

Pixel locations determined with CMM equipment to within 10 μm prior to installation in STAR

Programmed CMM Measurement method[#]:

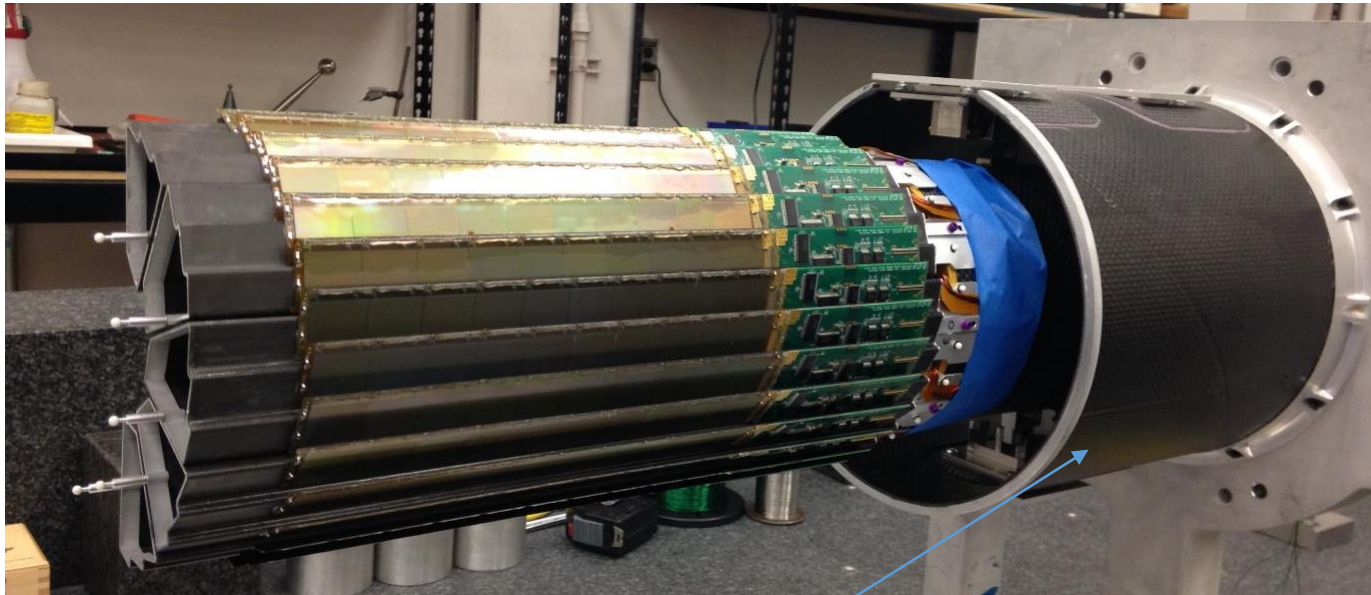
- All pixels located on a sector with respect to 3 sector tooling balls
 - 2 Lithography points on the chips measured with optical head
 - Chip surface profile measured with 11 x 11 point pattern using a Feather Probe*. Using a touch probe permits picking up over hung surfaces



PXL sensor surface profile from survey: $\pm 30 \mu\text{m}$ > PXL hit error, and the chip to chip surface deviation along the ladder surface is still larger, but all of this is then corrected with the spatial map

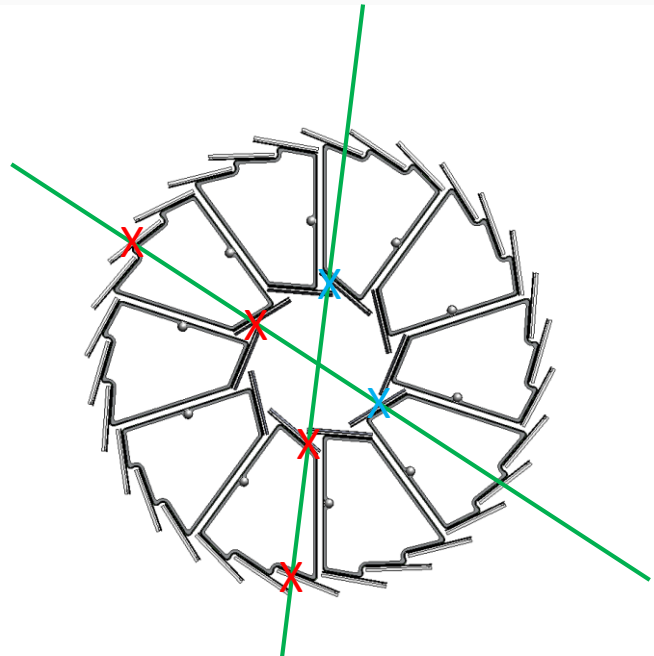
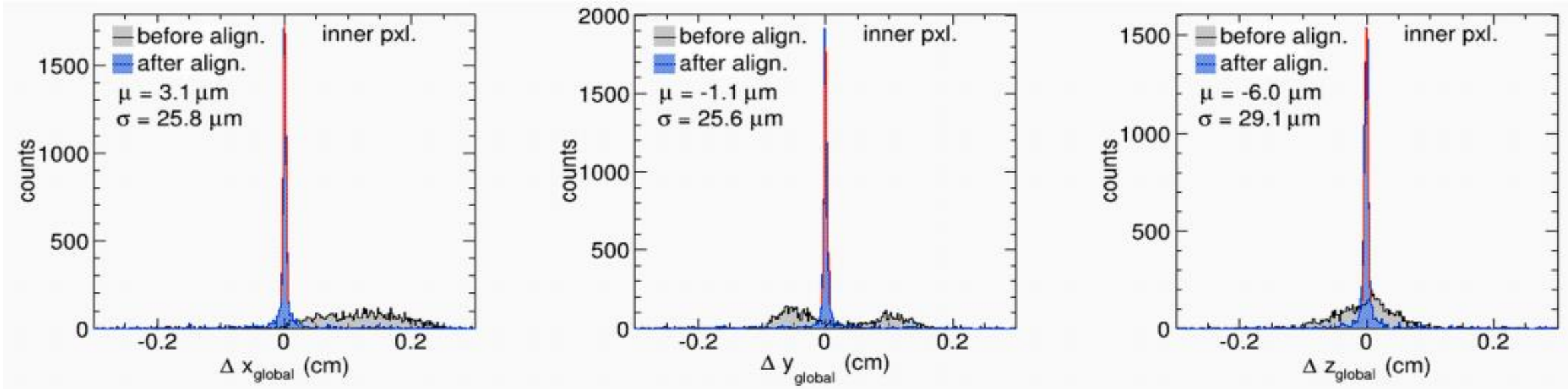
[#] For details: Hao Qiu HQiu@lbl.gov , Bob Connors RWConnors@lbl.gov
Full sector measurement takes ~ 8 hours

* Feather Probe, Optical Gaging Products (OGP), milligram level force, 1 mm ball
<http://www.ogpnet.com/ogpAccFeatherProbe.jsp?page=41>



- After assembling sectors in a half shell sector tooling balls measured with touch probe relative to kinematic mount coordinate frame
- Since the shells are supported the same way in the CMM and in the STAR installation the relative pixel position mapping is not disturbed

duplicate, truncated PXL support tube with kinematic mounts



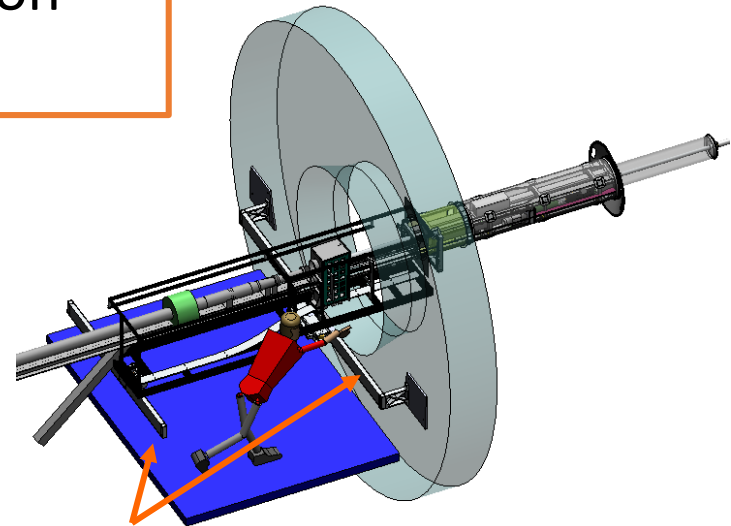
Cosmic ray result

Excellent half to half pointing, sub 30 μm

But after half to half alignment which was required to correct poor reproducibility of kinematic mount seating

Xs shows how hits are selected for projective distance of closest approach comparison

System for rapid PXL installation (external mechanics)



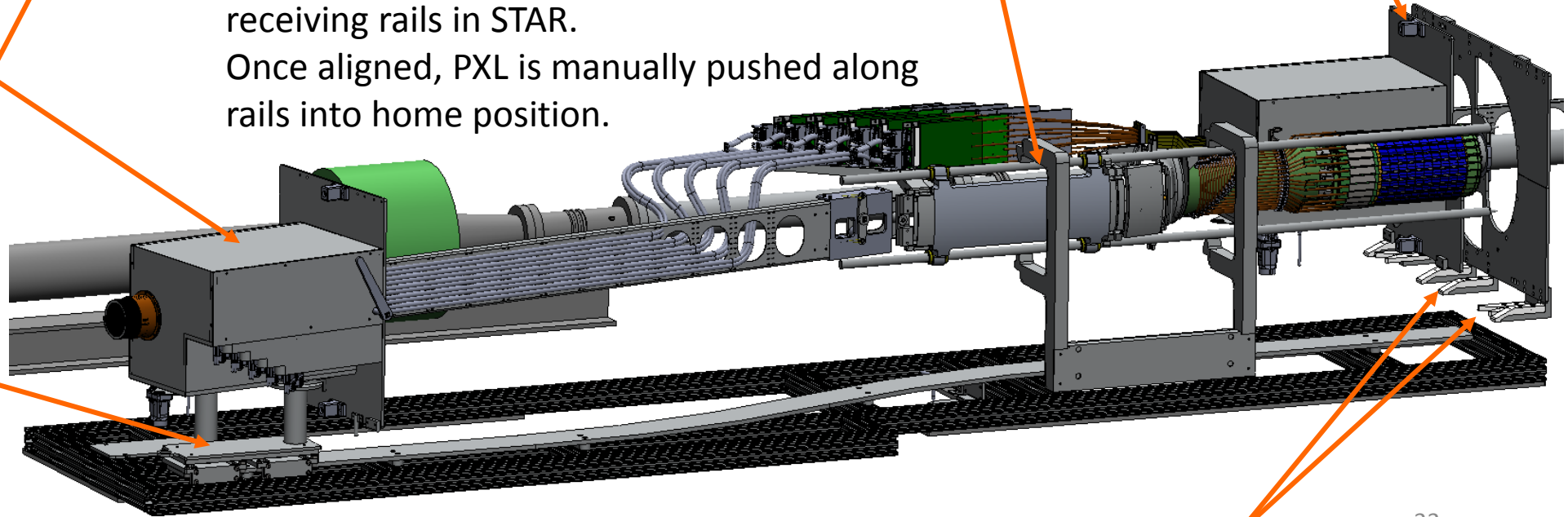
PXL carriage supported on slide rails in transport fixture

two captured screws, one top one bottom, secure and seal the bulkhead box to the detector housing

The 6 degree screw jack system, built into support, is used to align transport rails with receiving rails in STAR. Once aligned, PXL is manually pushed along rails into home position.

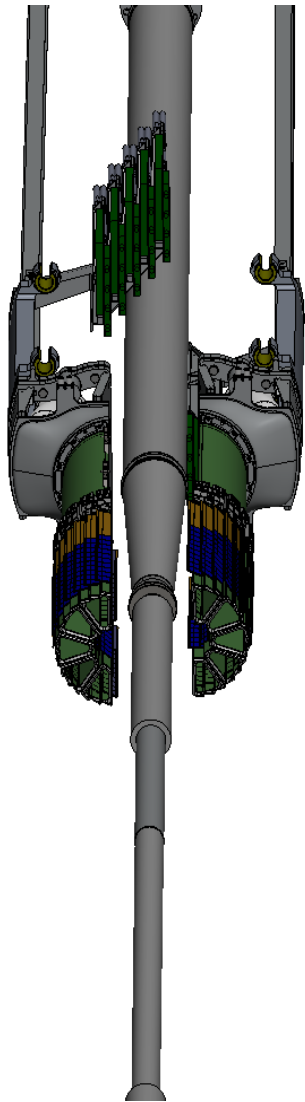
Bulkhead box with all electrical and air connections

Trolley guide to steer box around beam pipe elements

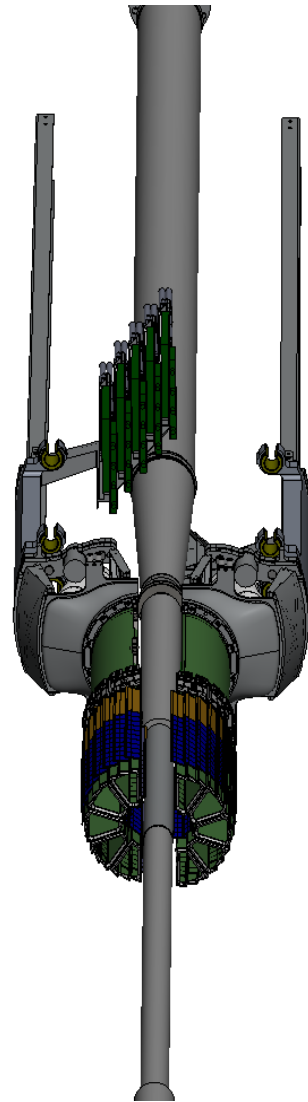


positioning guides to receive the bulkhead box

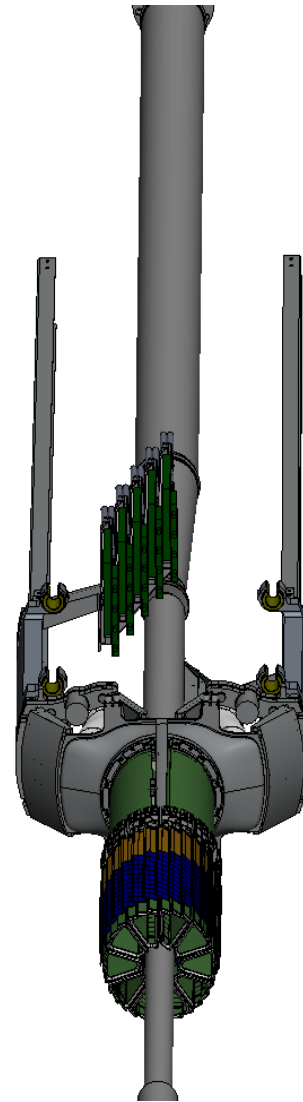
System for rapid PXL installation (internal mechanics)



open to clear beampipe
flanges



closing down



fully inserted and locked
in kinematic mounts

As the PXL detector slides into home position it starts open to clear larger beam pipe sections. It then successively closes down around the small beam pipe section and clears the narrowing outer containment tube.

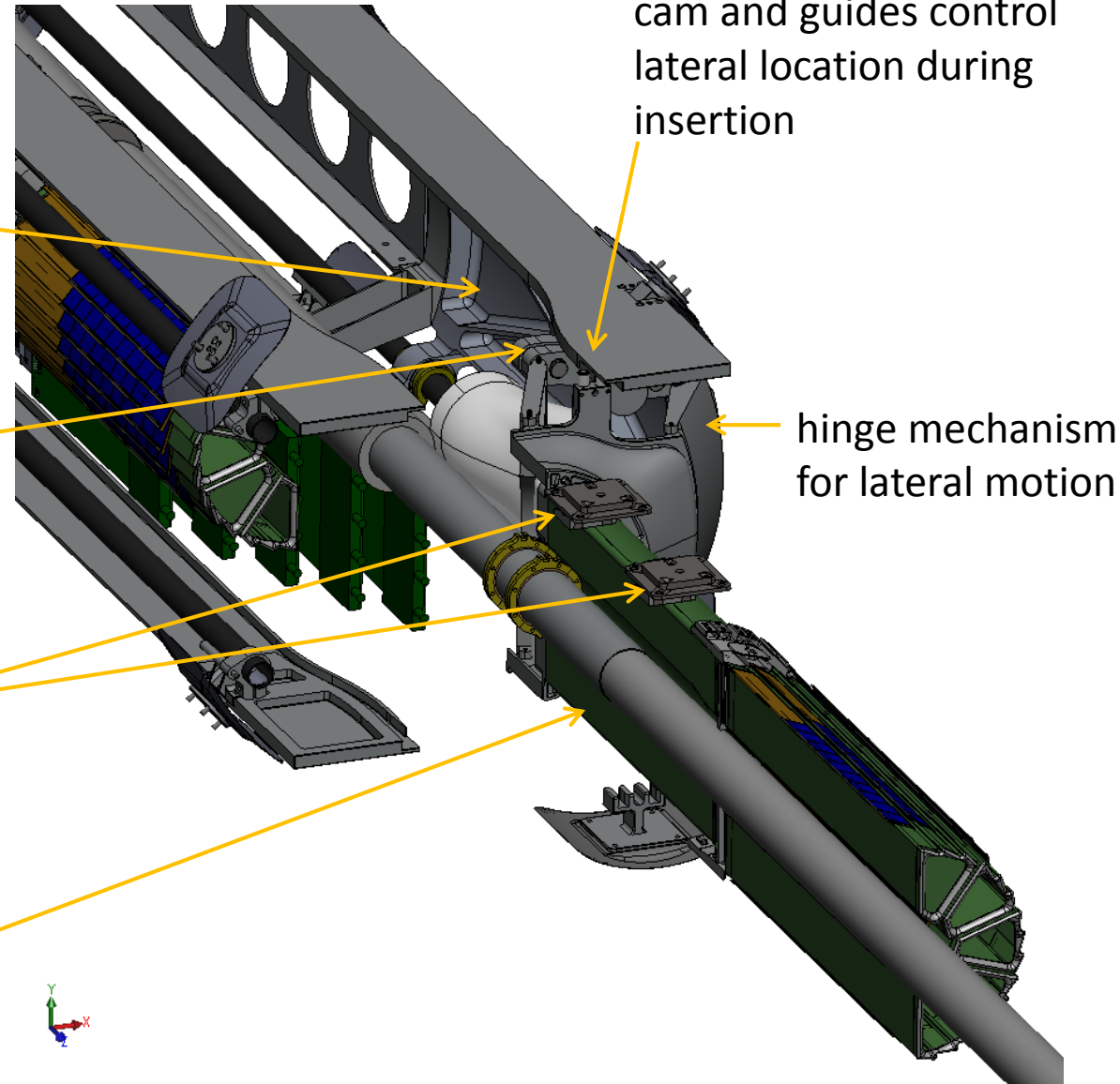
System for rapid PXL installation (internal mechanics)

carriage rides on support rails

mechanical release to transfer load to kinematic mounts

kinematic mounts engage at home position

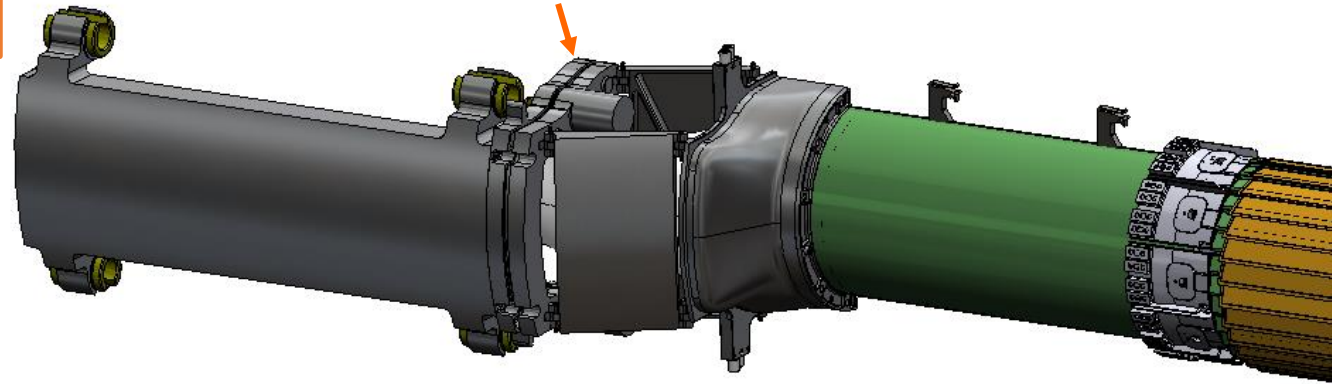
thin carbon half tube for PXL support and cooling air duct



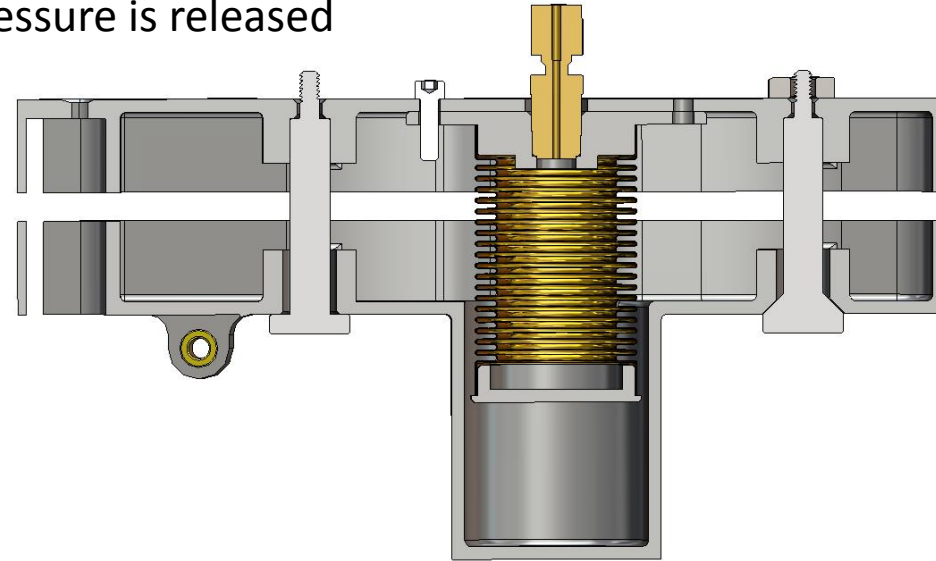
System for rapid PXL installation (internal mechanics)



Hold and release mechanism to transfer support from the rail carriage to the kinematic mounts



decouples carriage constraint when air pressure is released



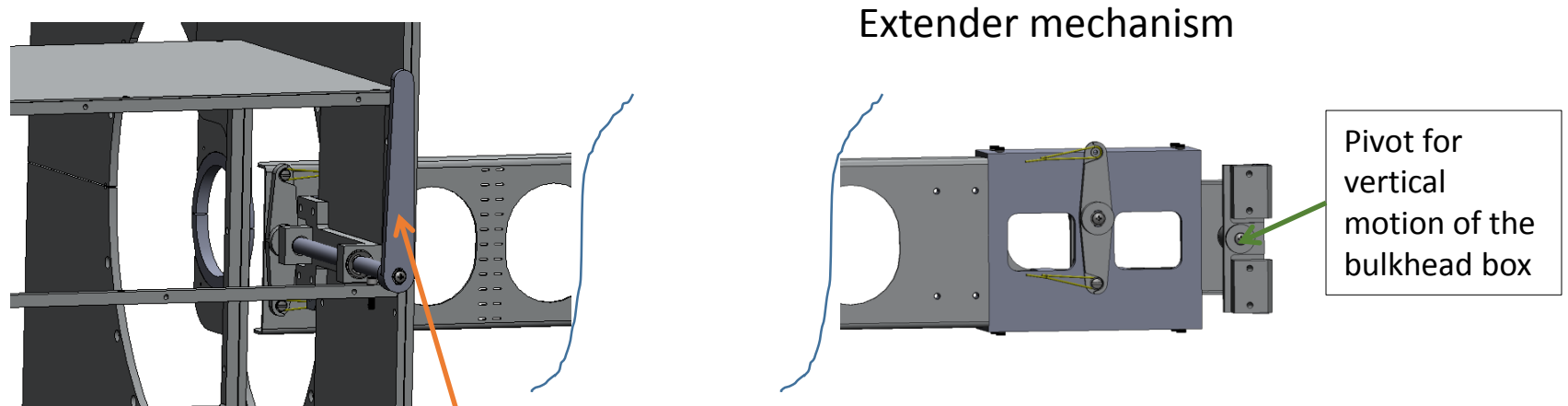
cross section view

bellows piston locks coupling under pressure

By setting the correct air pressure this system also limits the engagement force applied to the kinematic mount

System for rapid PXL installation (internal mechanics)

A lever actuated extender provides a reduced friction motion for the final engagement of the kinematic mounts. This allows better tactile feedback as the kinematic mount latches.

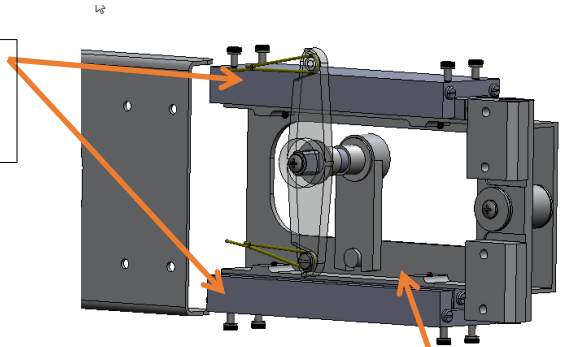


Extender mechanism

Pivot for vertical motion of the bulkhead box

Lever locate on the bulkhead box couples to extender with bronze cables.

Non magnetic linear bearings



Cam driven slide

HFT PXL detector

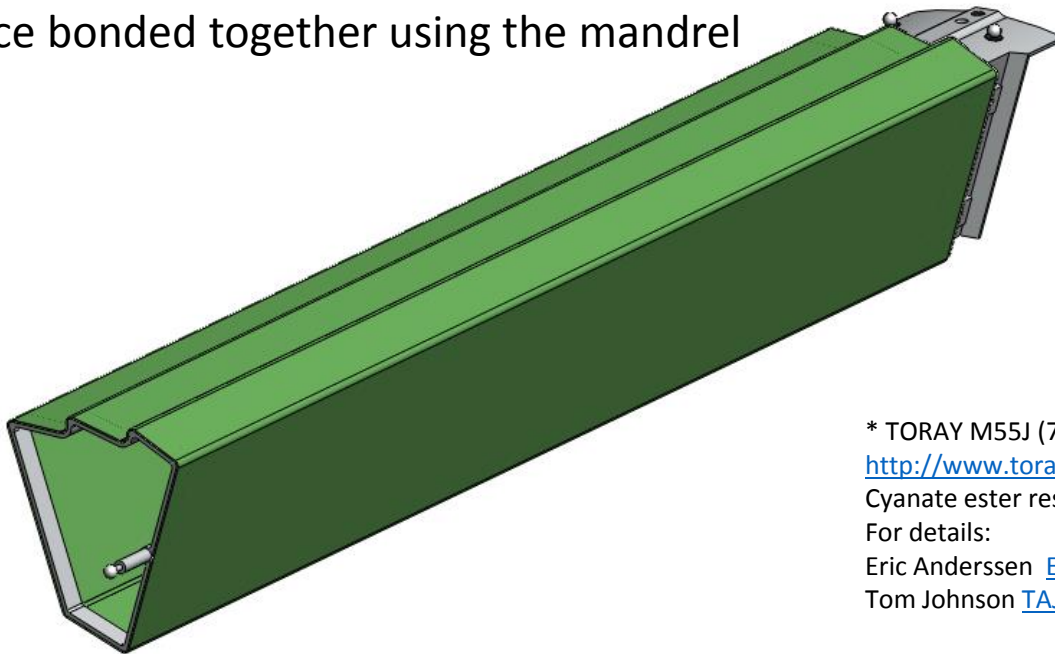
First MAPS based vertex
detector installed and
operating in STAR

end

Fabrication details

Stiff Carbon Composite Sector Tube, large moment of inertia

- 260 μm thick wall
- unidirectional carbon fiber with cyanate ester resins*
- 7 layer, 0,-60,+60,0,+60,-60,0 deg layup for reduced cure warpage
- Layup in two halves on an aluminum mandrel with caul plate control of inside radius features
- vacuum bagged and Autoclave cured
- 2 piece bonded together using the mandrel



* TORAY M55J (78 Msi/538 Gpa) PAN GRAPHITE/EX-1515

<http://www.toraycompam.com/>

Cyanate ester resin system, TenCate EX-1515 http://www.tencate.com/amer/Images/EX1515_DS_Web_05121429-3894.pdf

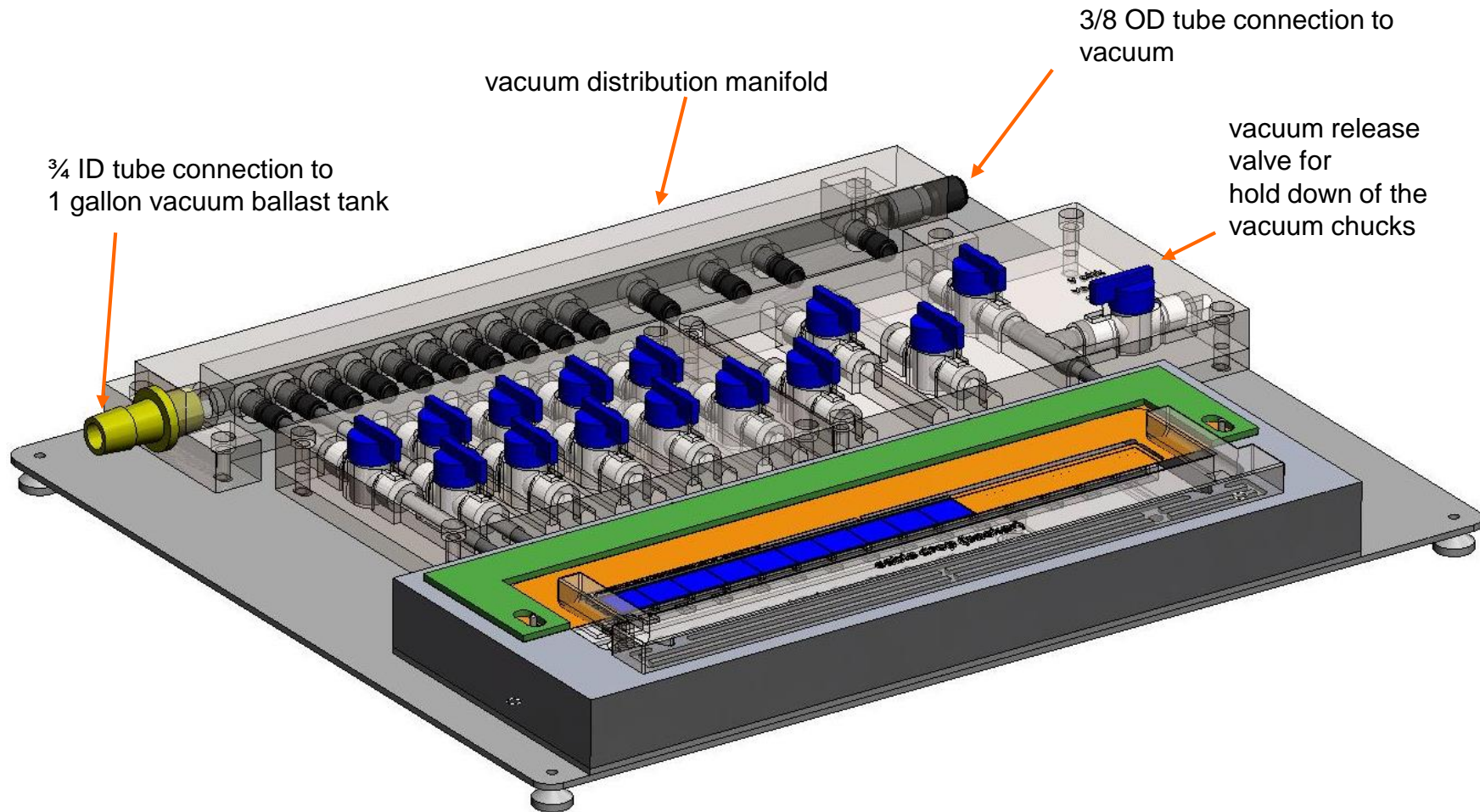
For details:

Eric Anderssen ECAnderssen@lbl.gov

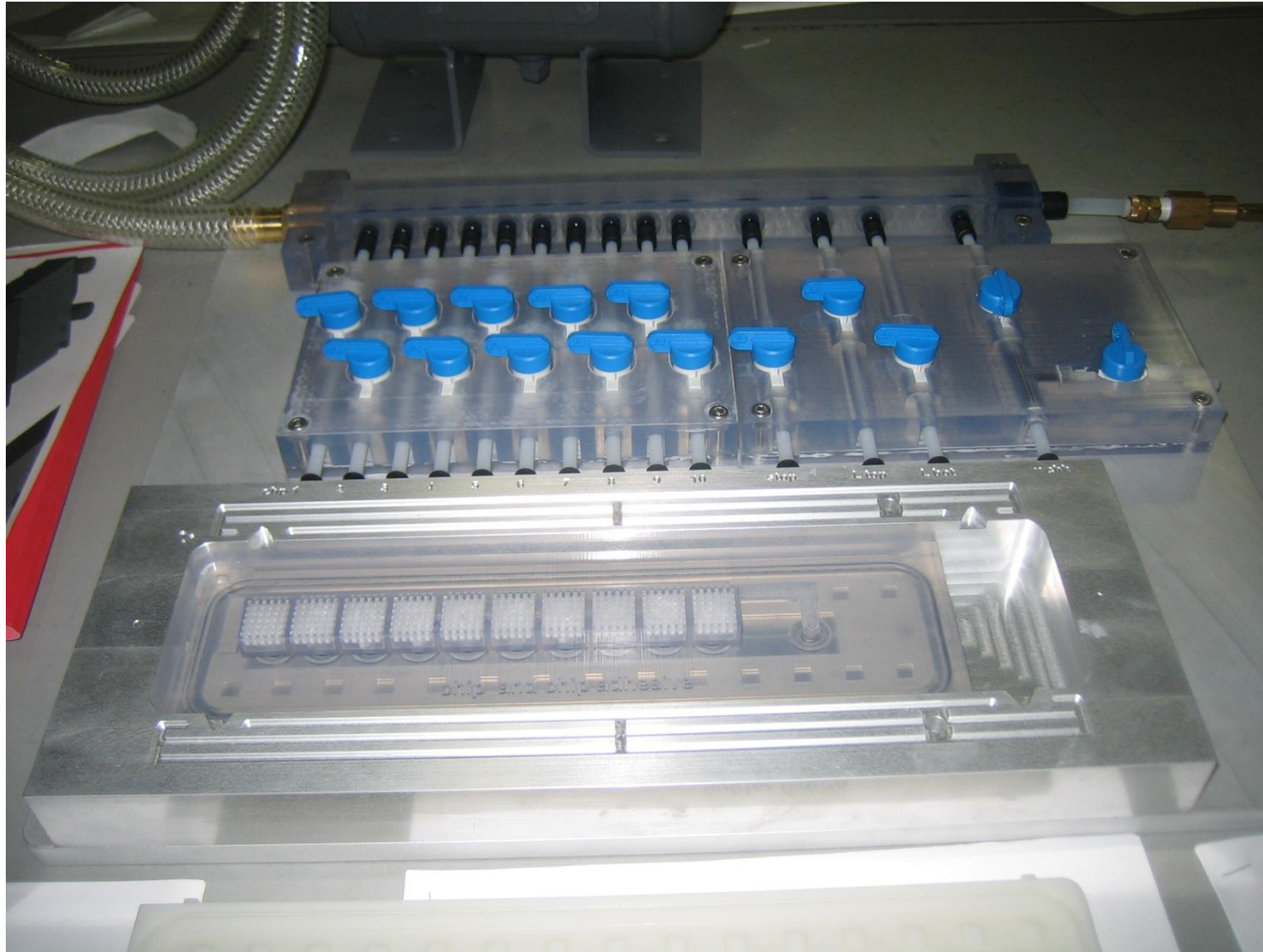
Tom Johnson TJohnson@lbl.gov

ladder assembly fixture

vacuum chuck system for placing chips and other ladder parts



Ladder assembly fixture



PXL Ladder Assembly



Precision vacuum chuck fixtures to position sensors by hand.

Sensors are positioned with butted edges. Acrylic adhesive prevents CTE difference based damage.

Weights taken at all assembly steps to track material and as QA.

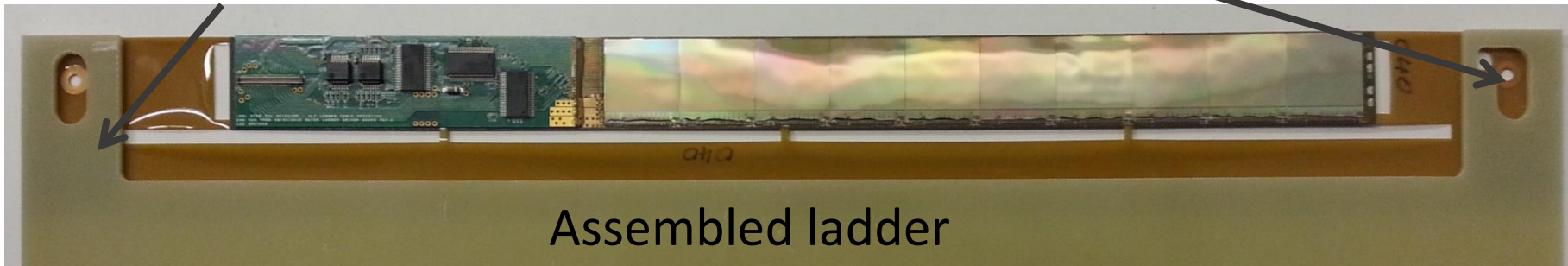
Hybrid cable with carbon fiber stiffener plate on back in position to glue on sensors.



Sensor positioning

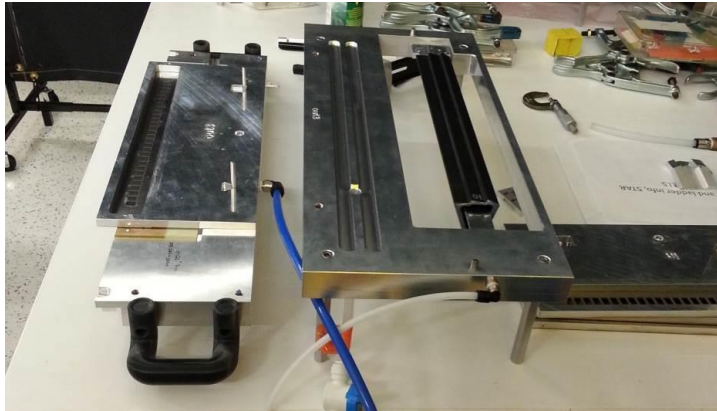
Cable reference holes for assembly

FR-4 Handler



Assembled ladder

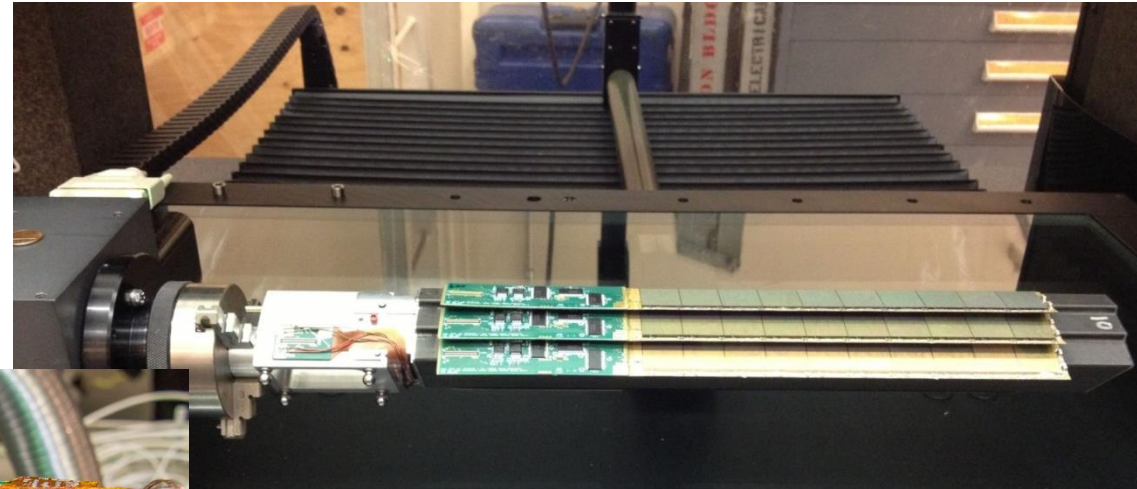
Sector and detector half assembly



Sector assembly fixture

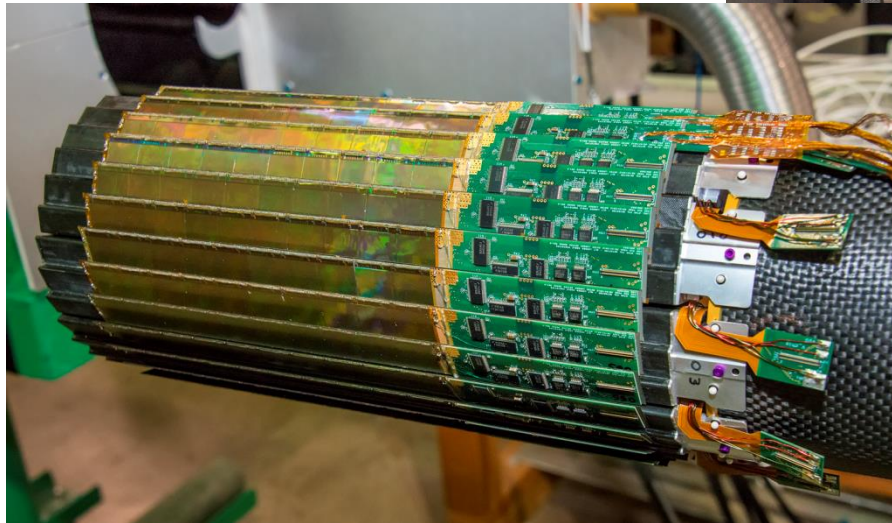
Sectors

- ▶ Ladders are glued on carbon fiber sector tubes in 4 steps
- ▶ Pixel positions on sector are measured and related to tooling balls
- ▶ After touch probe measurements, sectors are tested electrically for damage from metrology



Sector in the metrology setup

A detector half



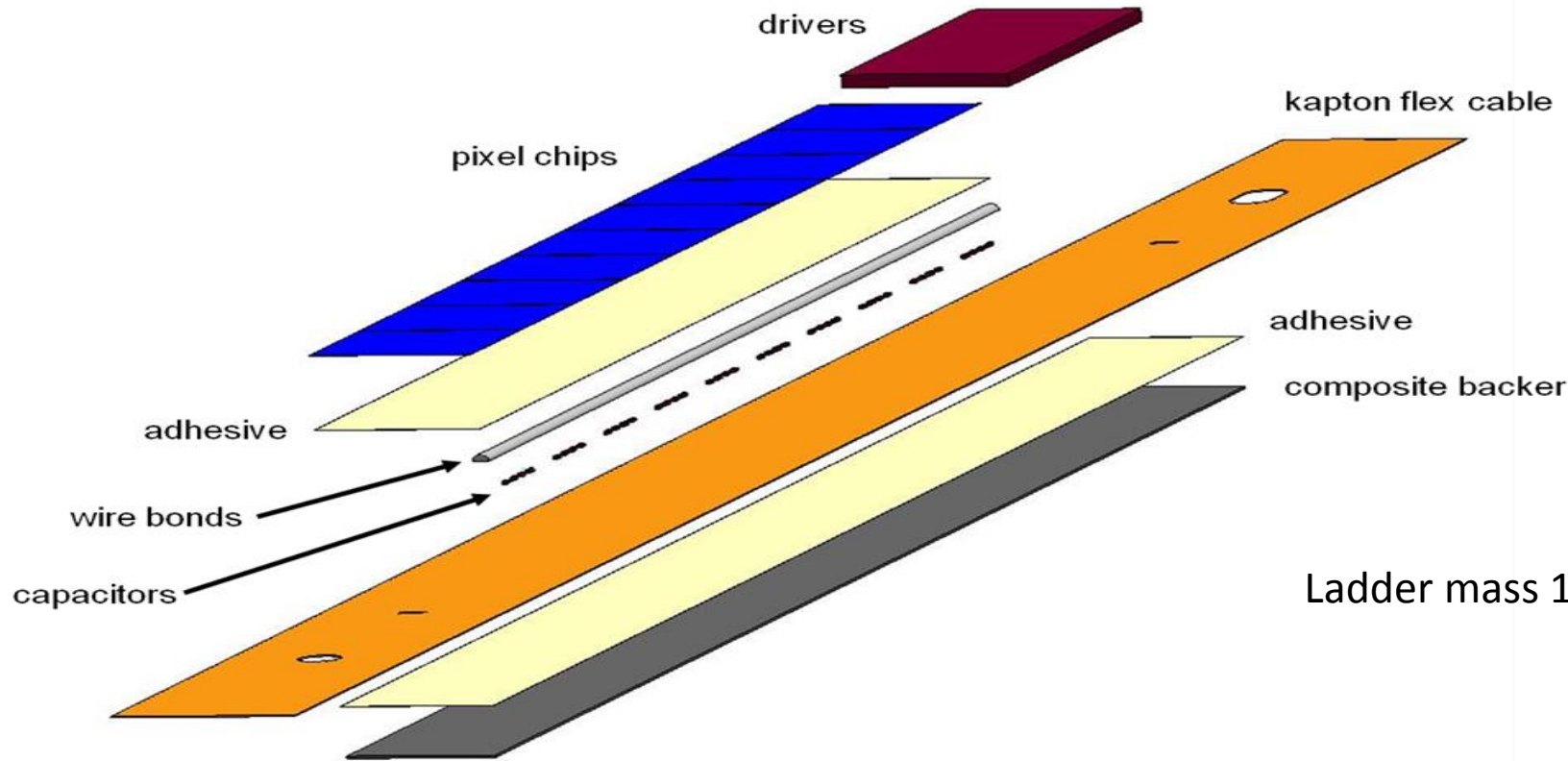
Detector half

- ▶ Sectors are mounted in dovetail slots on detector half
- ▶ Metrology is done to relate sector tooling balls to each other and to kinematic mounts → Detector half mapped

extra material



Ladder construction

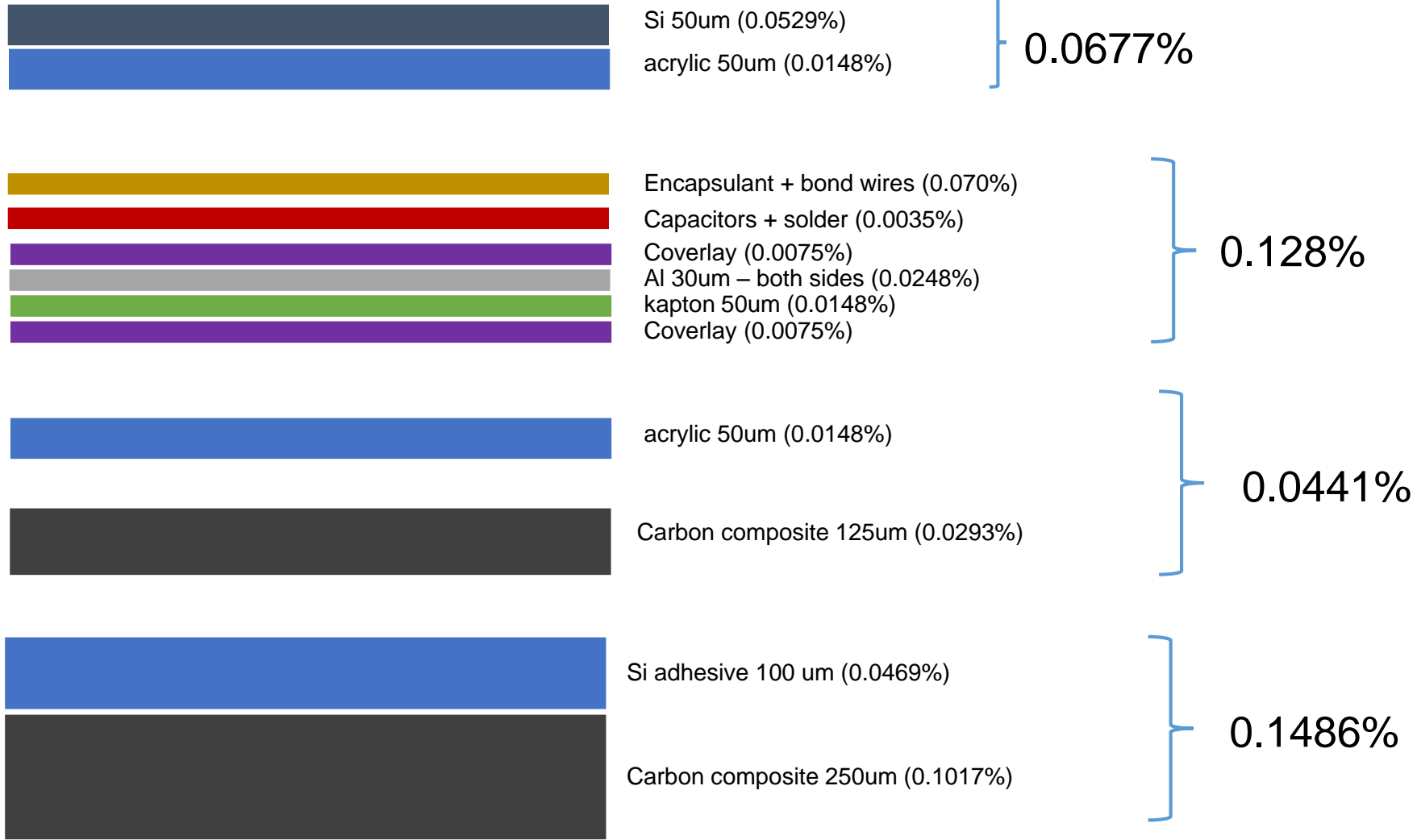


Soft sheet adhesive
 3M 467MP 200MP adhesive,
 acrylic 2 mil sheet, shear
 modulus 1.5×10^4 Pa (2 psi)



Ladder mass 11.6 grams

Radiation length in low mass area

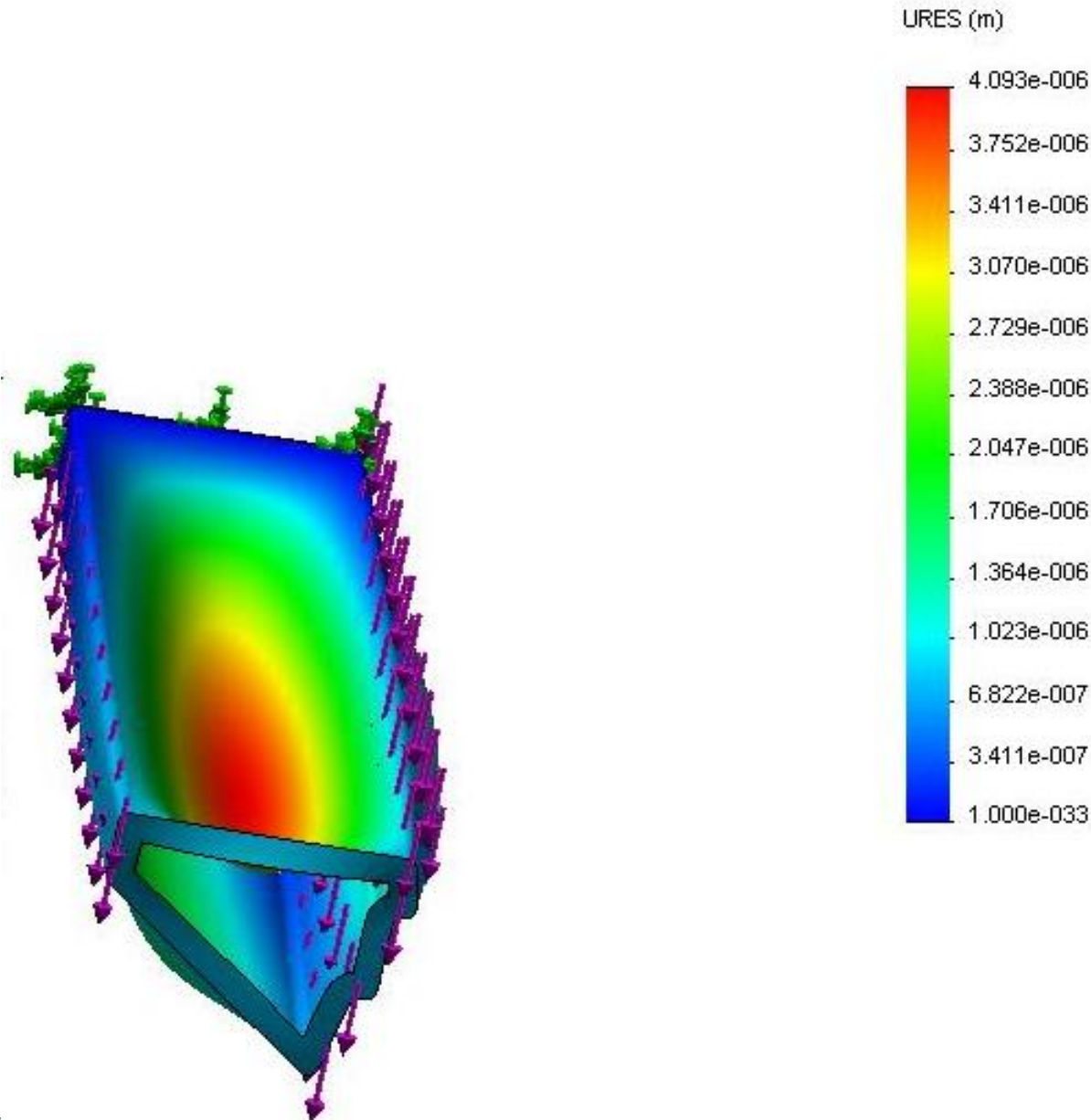


Total = 0.388%

NOTE: Does not include sector tube side walls

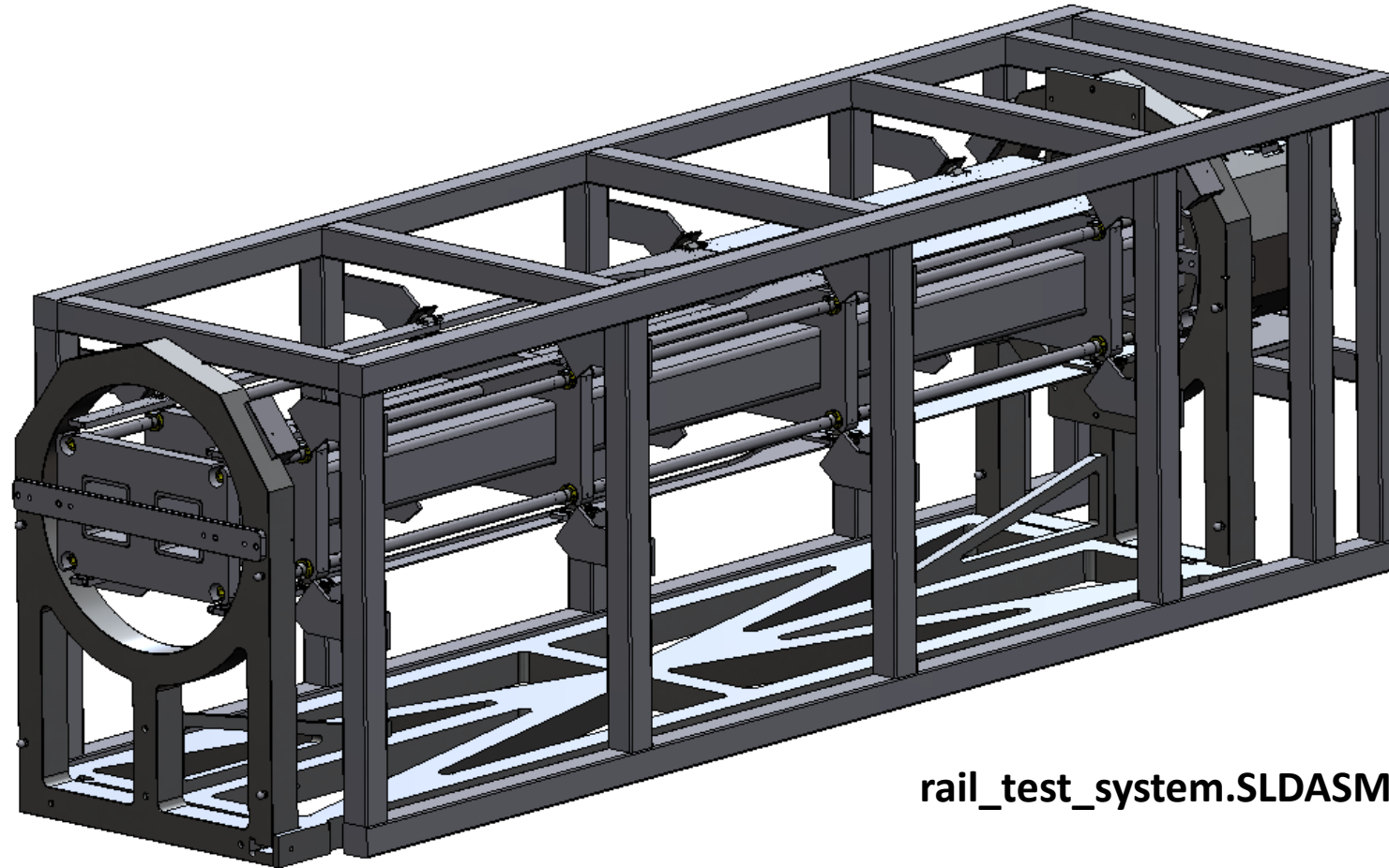
from older estimate

FEA analysis - sector beam deformation – gravity load



- FEA shell analysis
- 120 micron wall thickness composite beam
- gravity load includes ladders
- maximum structure deformation 4 microns
- ladder deformation only 0.6 microns

rail test system



rail_test_system.SLDASM

5/3/2010

this document: [http://www-rnc.lbl.gov/~wieman/Rail test system.pptx](http://www-rnc.lbl.gov/~wieman/Rail%20test%20system.pptx)

models: [http://www-rnc.lbl.gov/~wieman/rail test system 05 03 10.zip](http://www-rnc.lbl.gov/~wieman/rail%20test%20system%2005%2003%2010.zip)

Example tolerance spec

±0.05 mm tolerances are to preserve glue bond thicknesses

this and other 2 similar planes tolerances to chord and axis of ref cylinder: ±0.05 mm

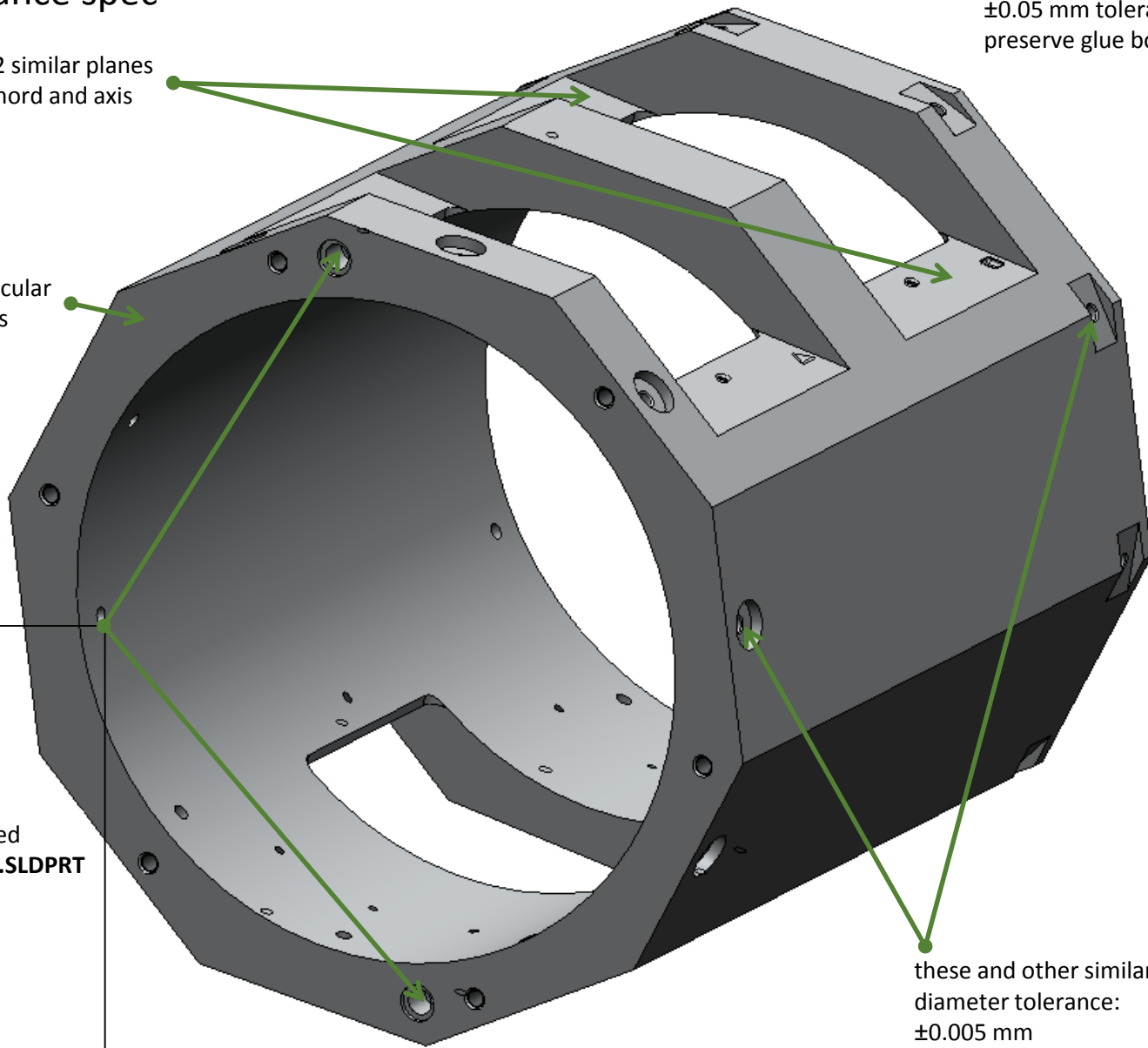
this plane perpendicular to a ref cylinder axis

line between holes centered on ref cylinder axis to ±0.05 mm

separation tolerance ±0.05 mm or match drilled with **butch_plate_single.SLDPRT**

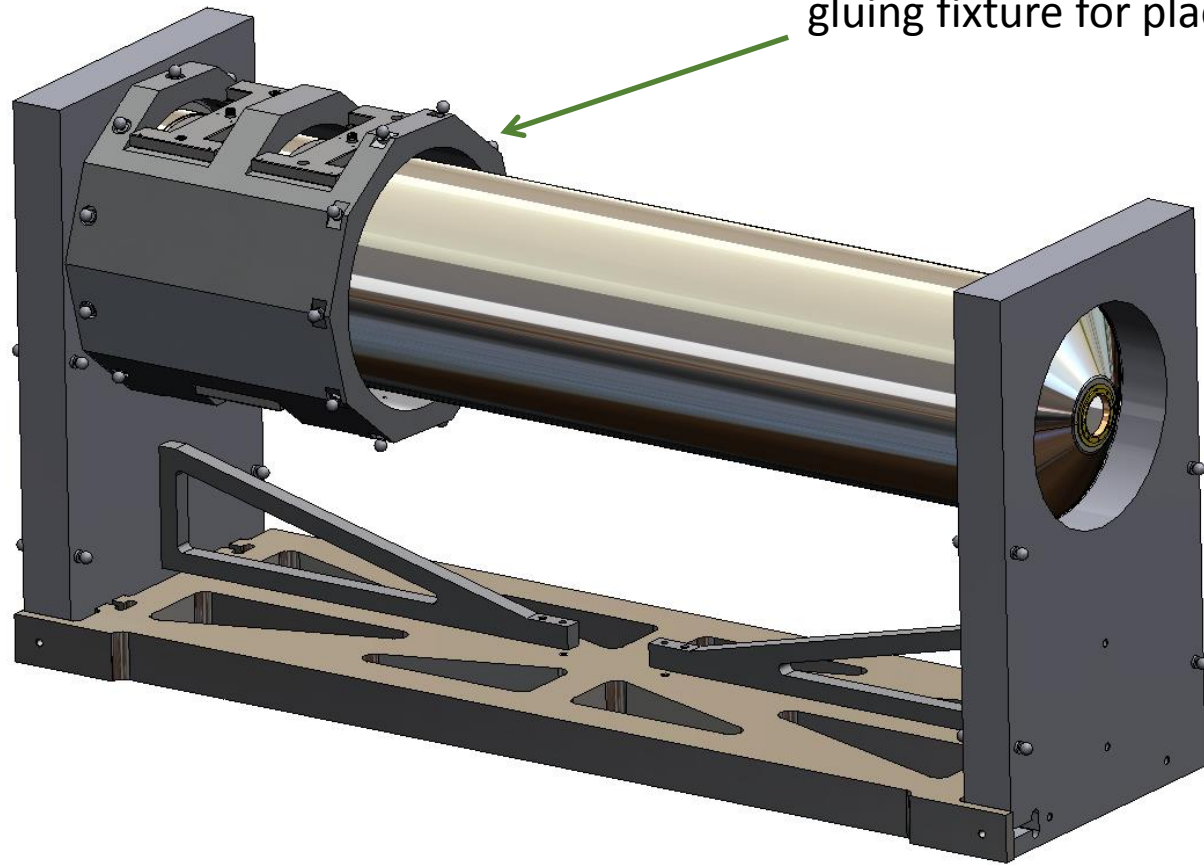
diameter tolerance:
+0.000 mm
-0.005 mm
for bullet insert press fit

these and other similar holes diameter tolerance: ±0.005 mm for press fit with tooling balls, glue in OK if ends up sloppy



grand_master.SLDPRT

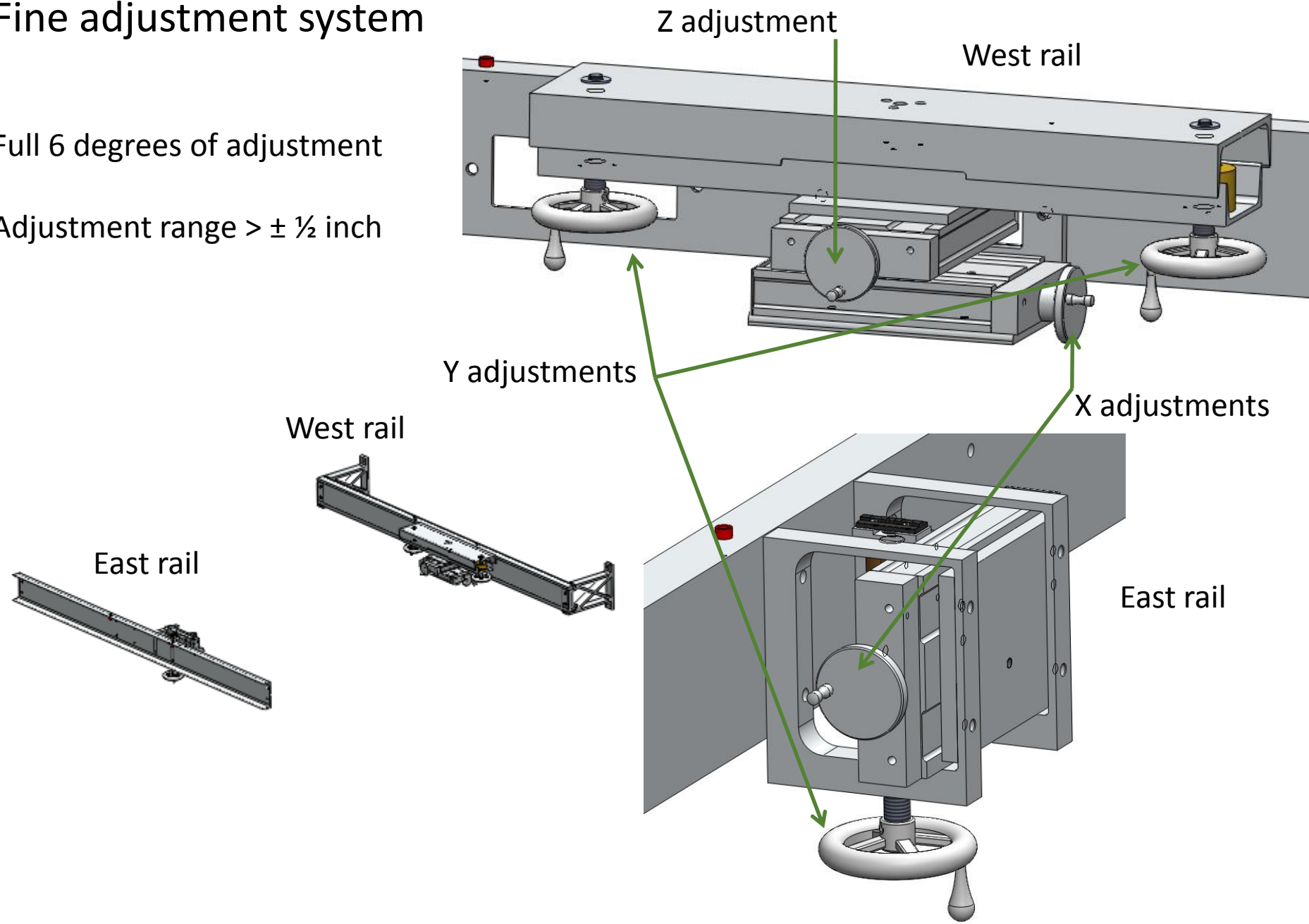
gluing fixture for placing kinematic mounts in PST

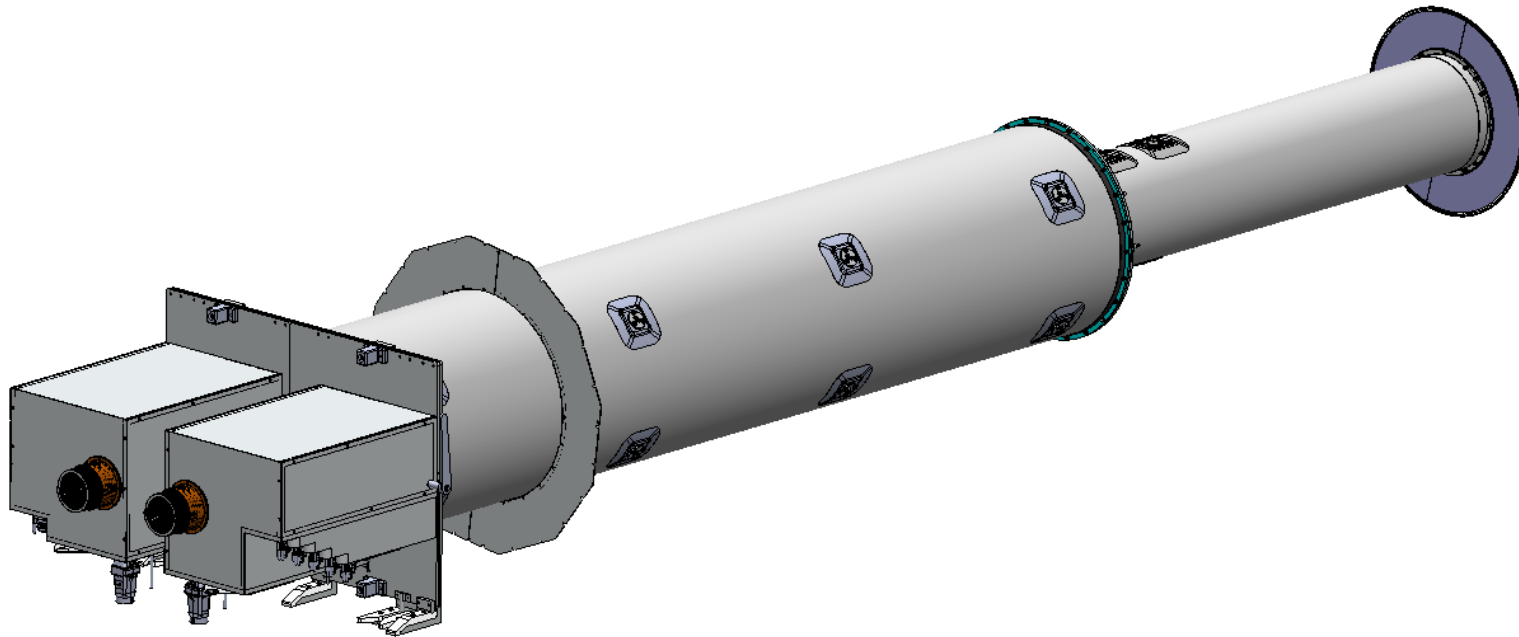


Fine adjustment system

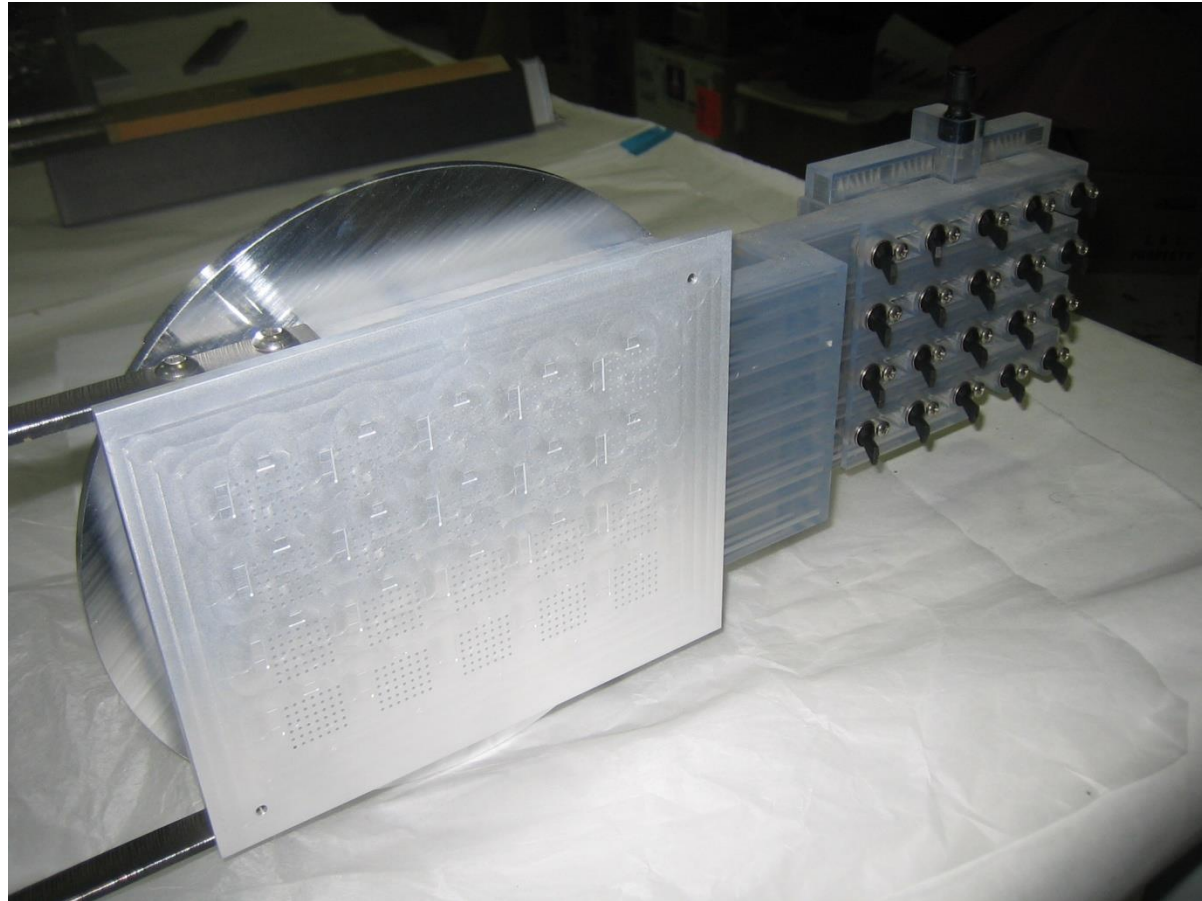
Full 6 degrees of adjustment

Adjustment range $> \pm \frac{1}{2}$ inch





vacuum chuck for thinned silicon chips in the probe station.
 plumbing done with rapid prototyping and cartridge valves



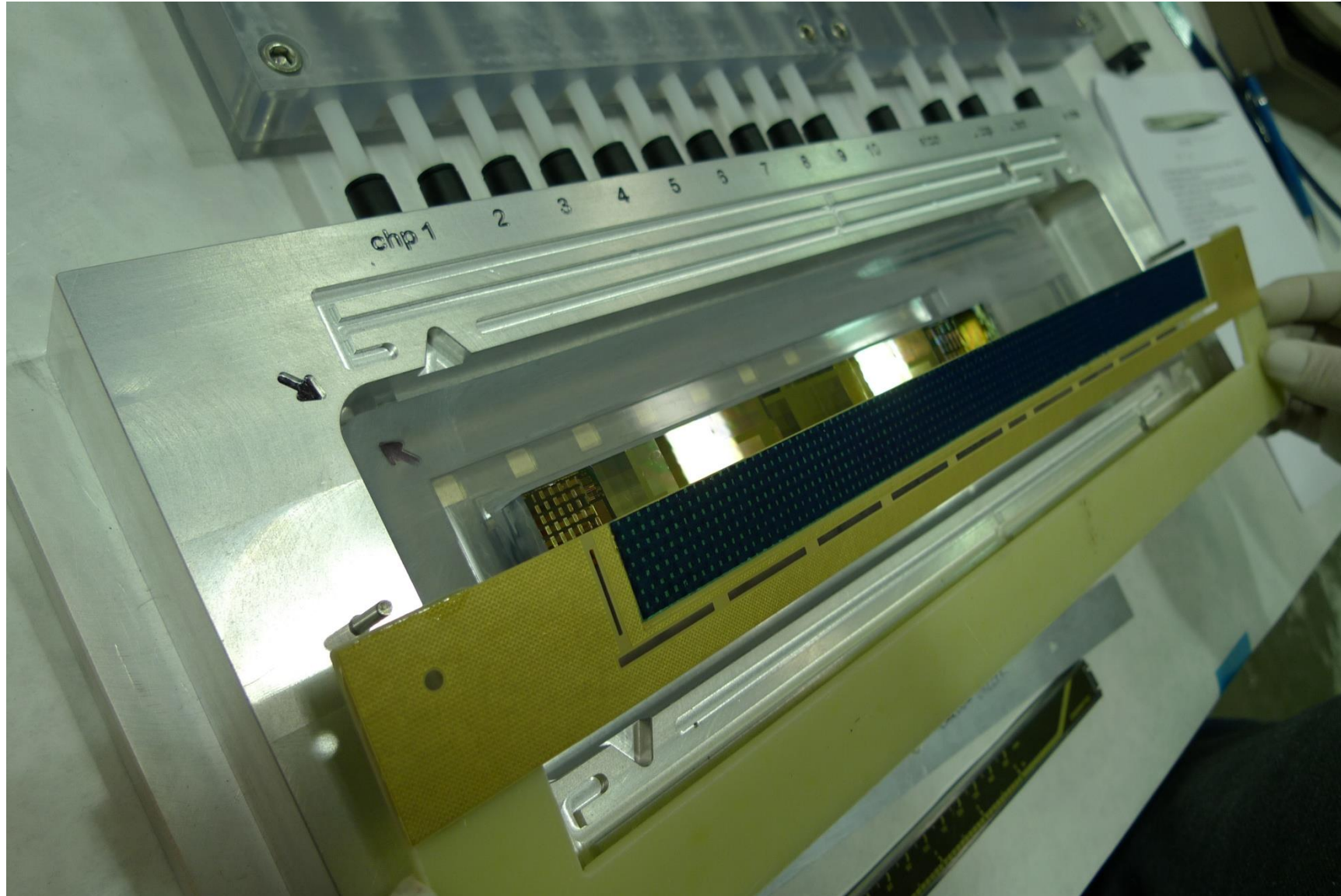
ladder fabrication and tooling



ladder fabrication and tooling

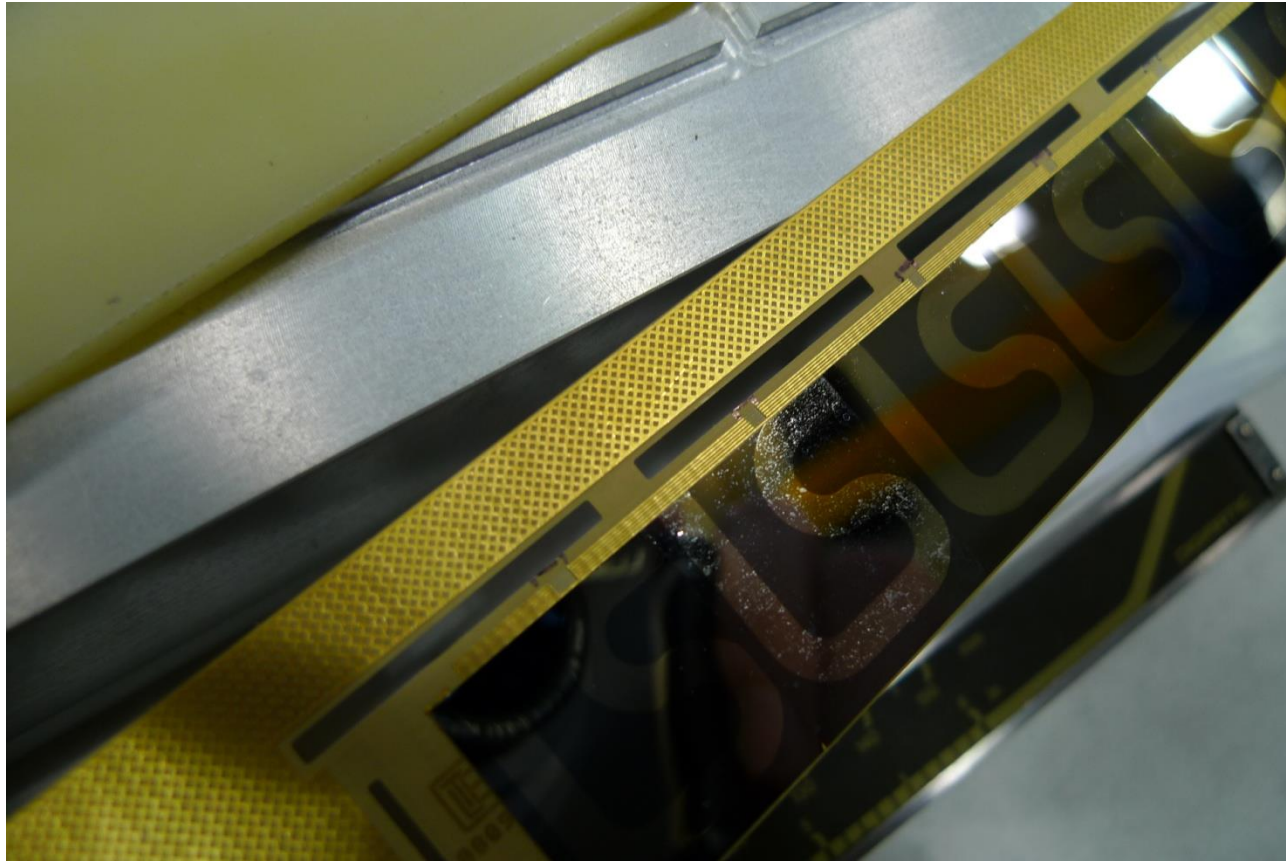


ladder fabrication and tooling



finalizing mechanical designs and developing rapid production methods

ladder fabrication and tooling



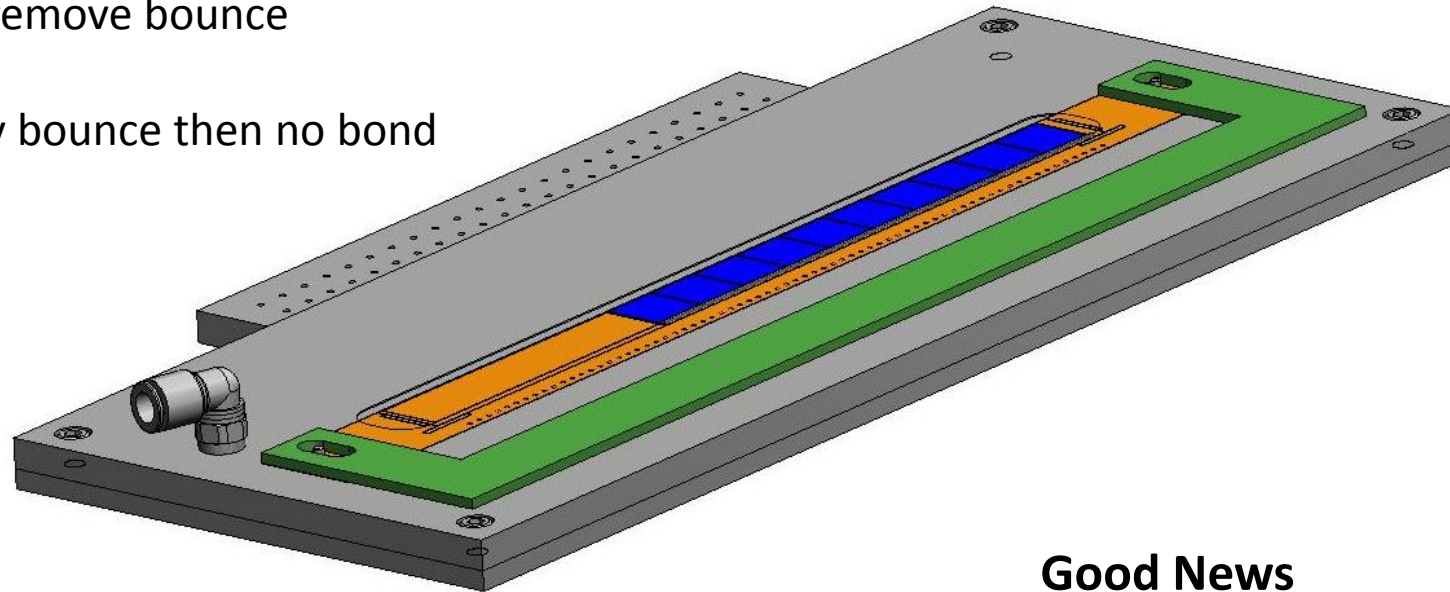
ladder with
silicon heater
chips
(50 μm thick)



wire bonding 50 μm silicon to flex PC

vacuum chuck to
secure flex and silicon
flat against solid surface
to remove bounce

Any bounce then no bond

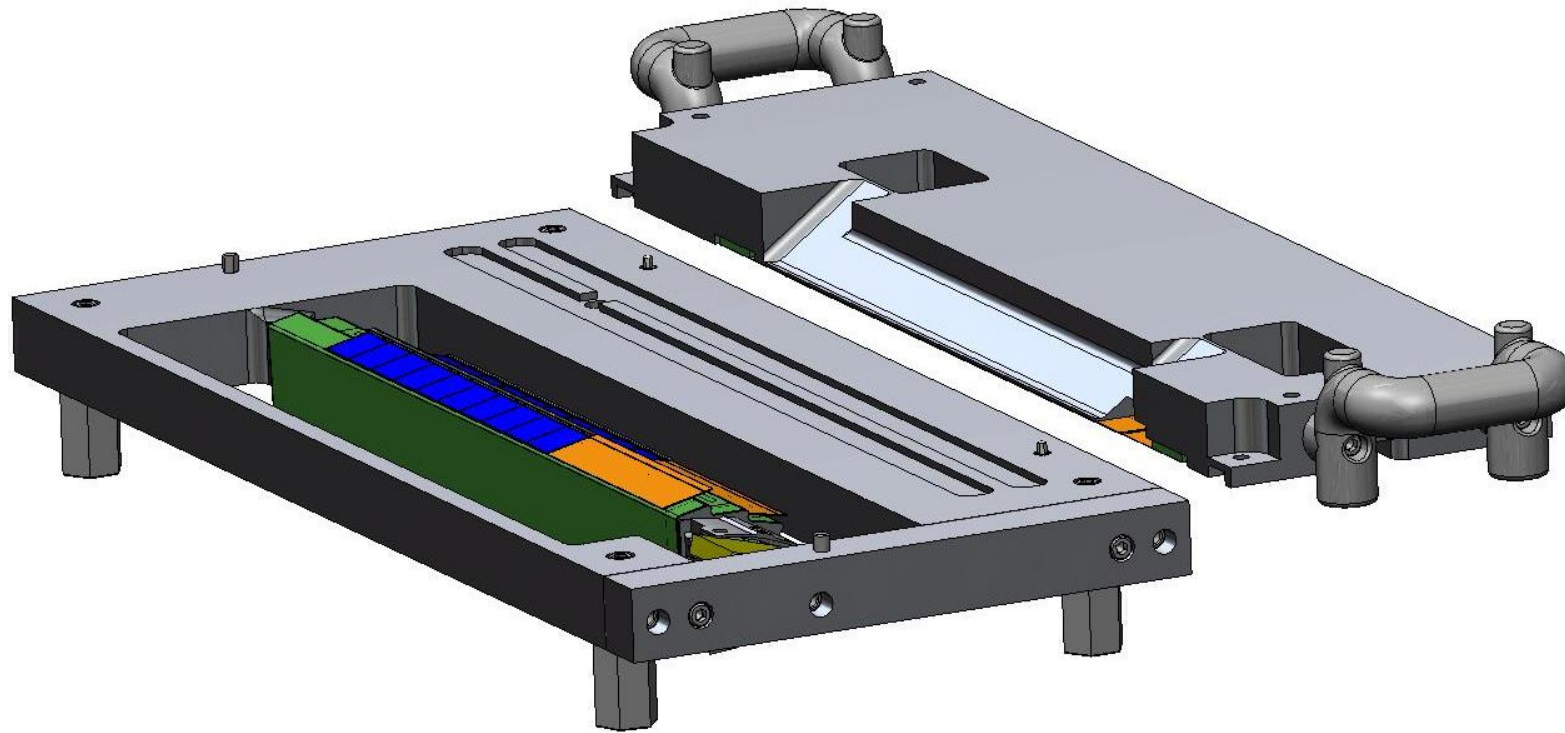


Good News

after a couple of minor
modifications to the vacuum
chuck wire bonding works well

fixture

(designed to allow ladder replacement)



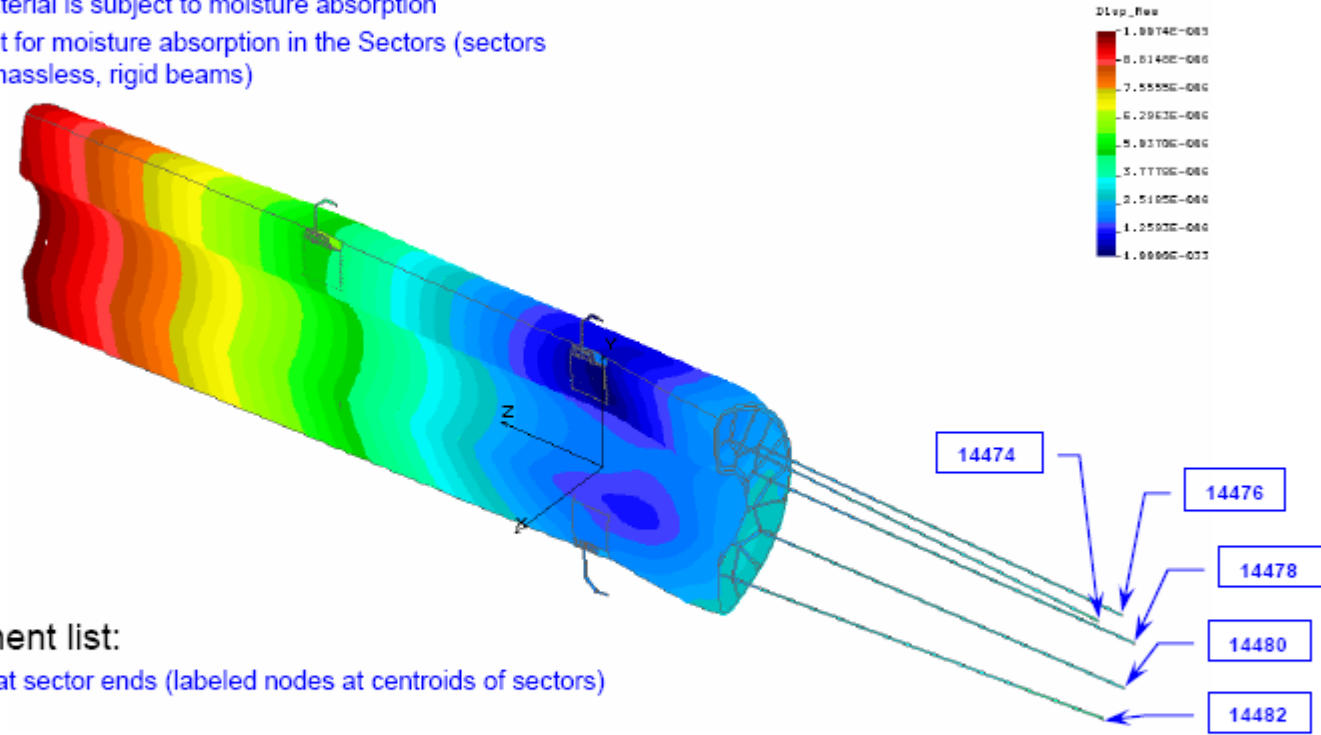
ladder to out2 bond fixture.SLDASM

ladder to sector tooling fixtures (4 stations)



D-Tube FEA – Displacements from Moisture Absorption

- Resultant displacements due to Moisture absorption:
 - Only YSH-50 material is subject to moisture absorption
 - Does not account for moisture absorption in the Sectors (sectors represented as massless, rigid beams)

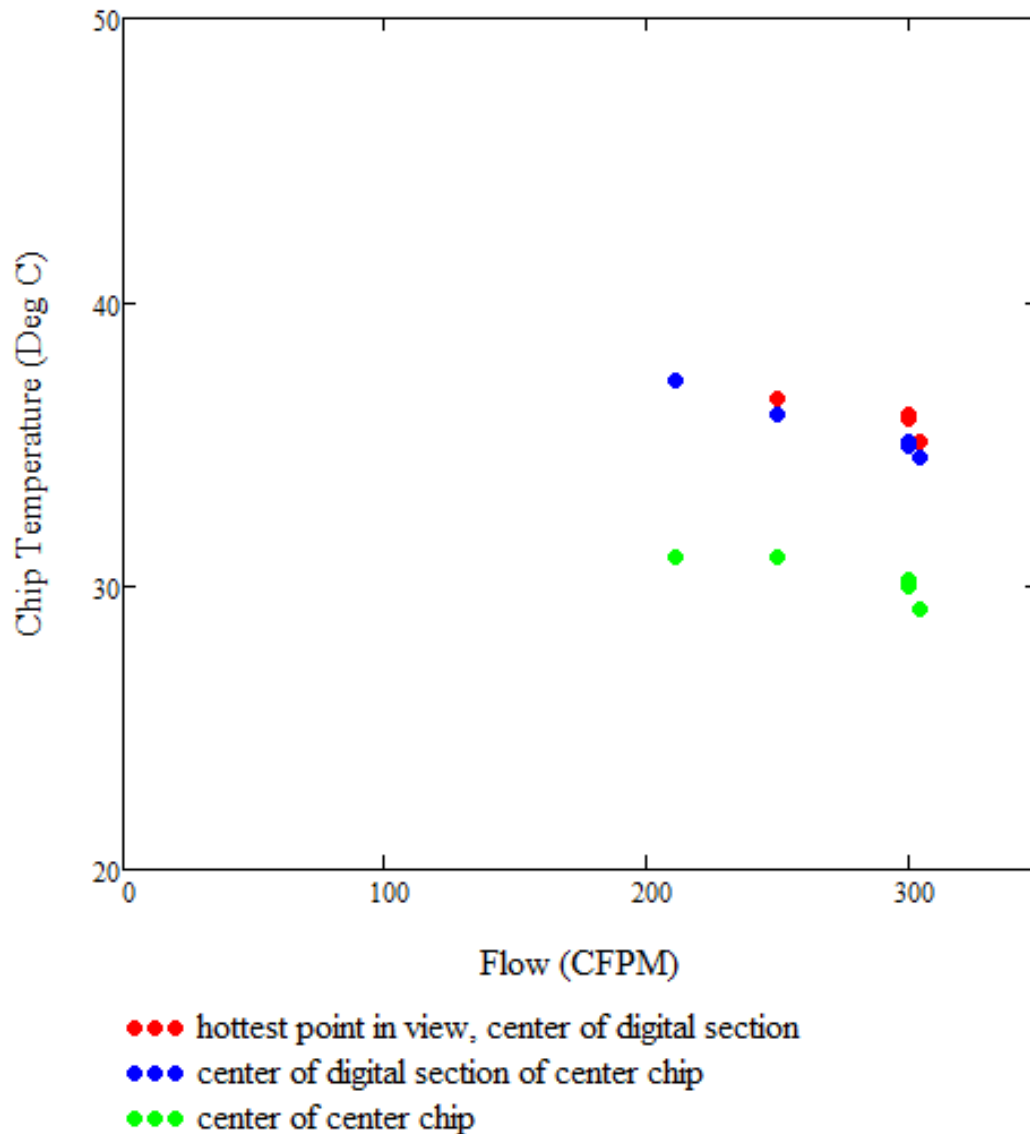


- Nodal-displacement list:
 - Displacements at sector ends (labeled nodes at centroids of sectors)
 - Units in meters

* Selection List 1	Load case 1					
Node	UX	UY	UZ	RX	RY	RZ
14474	1.491e-006	-2.641e-006	-1.957e-006	-8.095e-006	-3.184e-006	-3.940e-006
14476	2.287e-006	-5.054e-007	-2.143e-006	-3.984e-007	-7.055e-006	-4.012e-006
14478	1.997e-006	3.264e-007	-2.270e-006	2.994e-006	-6.523e-006	-3.212e-006
14480	2.071e-006	1.190e-006	-2.318e-006	6.510e-006	-6.420e-006	-2.465e-006
14482	1.070e-006	2.936e-006	-2.270e-006	1.238e-005	-2.083e-006	-7.713e-006



Measured silicon temperature as a function of cooling air flow



The air flow in STAR as of February 2014 is 340 CFPM. So, the hottest point on the chip should be less than 35 deg C and the temperature in the pixel region of the chip should be less than 30 deg C.

The chip diode temperature is only read out on the eastern most end of the ladder. To within the accuracy of the measurement no temperature change is observed between ladder power on and ladder power off.

Log book reference:

<https://skydrive.live.com/redir?page=view&resid=C9B8662B3A1439D3!548&authkey=!AG8fPDrdLvjbyZ0&wd=target%28PXL%20thermal.one%7c4D40E4DD-B650-49FB-B343-E4BF32A476D8%2fThermal%20with%20ECU%20fully%20connected%7c7DF36A31-D948-4DCF-87B1-BC168D5DE3CF%2f%29>

capacitive probe

<http://www.lionprecision.com/>

LION
PRECISION
ISO9001 CERTIFIED

System Components

Probe Model: C1-A
Probe Serial: 030937-10
Driver Model: DMT20
Driver Serial: 031054-02
Channel: 0
Sensitivity Switch: NA

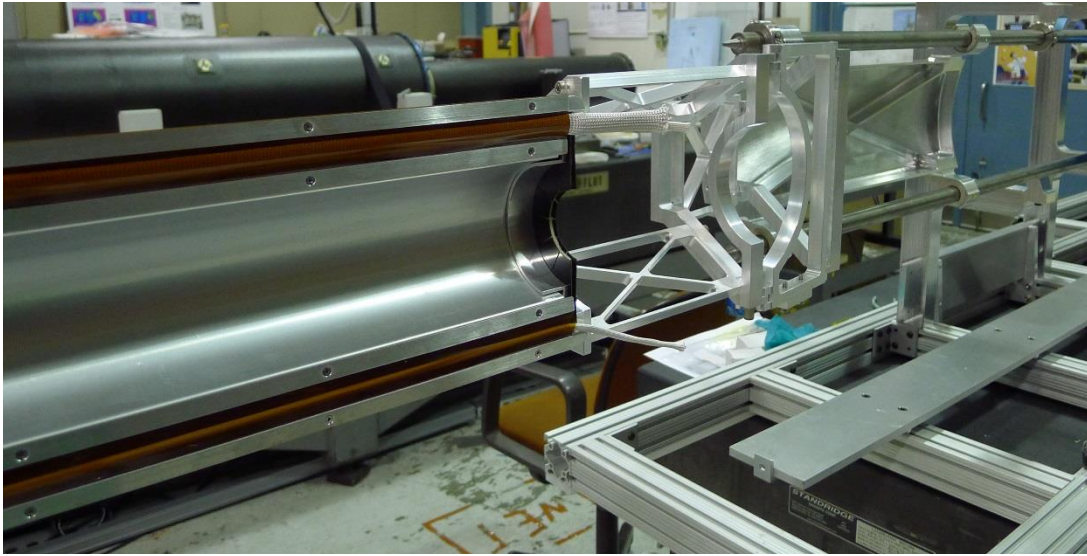
Peak to Peak Resolution: 50.0 nm
RMS Resolution: 2.0 nm

Report for Lawrence Berkeley Lab

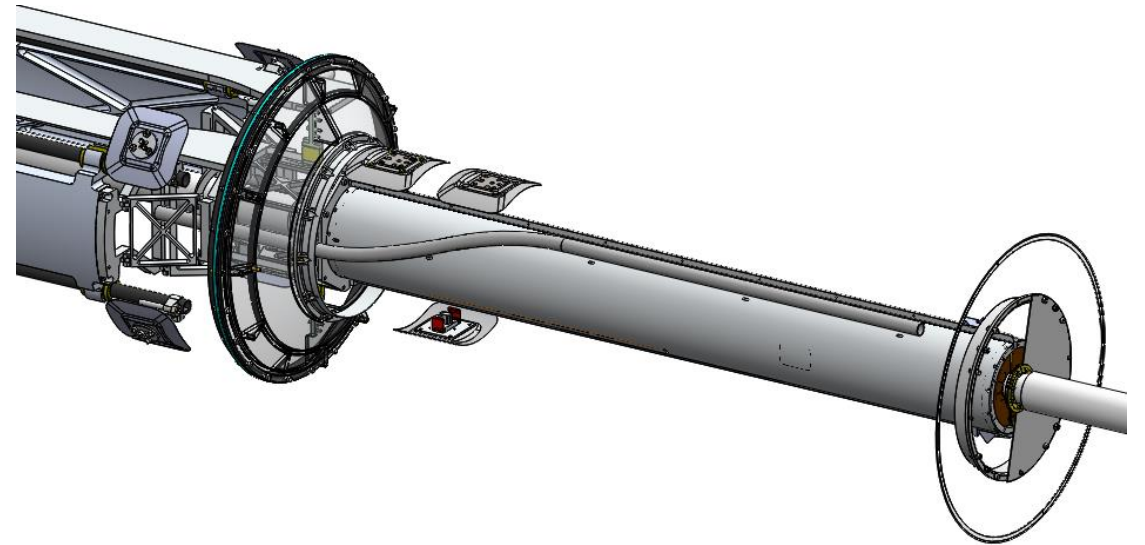
Order ID: 46873
Customer ID: 2025
Calibration Date: 1/15/2004
Calibration Due Date: 1/14/2005
Calibration Number: 2456

Calibration Parameters

Range: 500 μm
Standoff (range center): 750 μm
Output Voltage: 10 to -10 VDC
Output Sensitivity: 0.04 V/ μm
Target: flat target
Bandwidth (-3dB): 20000 Hz



Insertable bake out jacket for the central portion of the beam pipe



2. Probability for picking the correct hit with an infinite search window using the chi-squared method

$$P_{\text{ch}} = \frac{1}{2 \cdot \pi \cdot \sigma_x \cdot \sigma_y \cdot \rho + 1} \quad \text{eq. 2}$$

Note, as expected eq. 1 reduces to the [closest hit form](#) when $\sigma_x = \sigma_y$

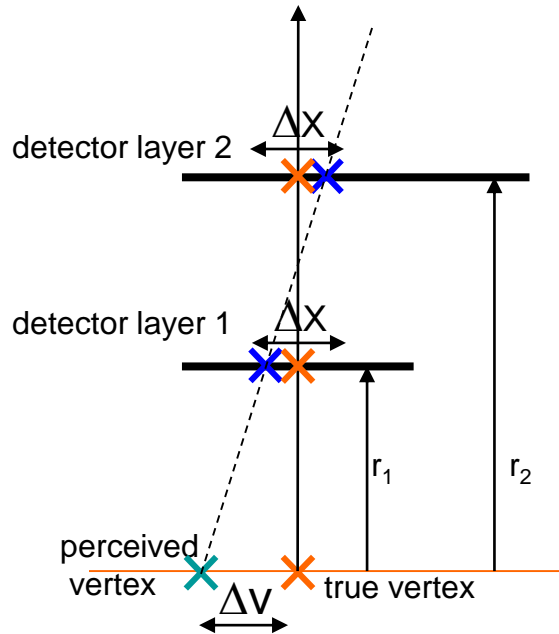
vertex projection from two points

expectations for the HFT pixels

$$\text{pointing resolution} = (13 \oplus 19\text{GeV}/p \cdot c) \mu\text{m}$$

from
detector
position
error

$$\Delta v = \Delta x \cdot \frac{\sqrt{r_2^2 + r_1^2}}{(r_2 - r_1)^2}$$



from
coulomb
scattering

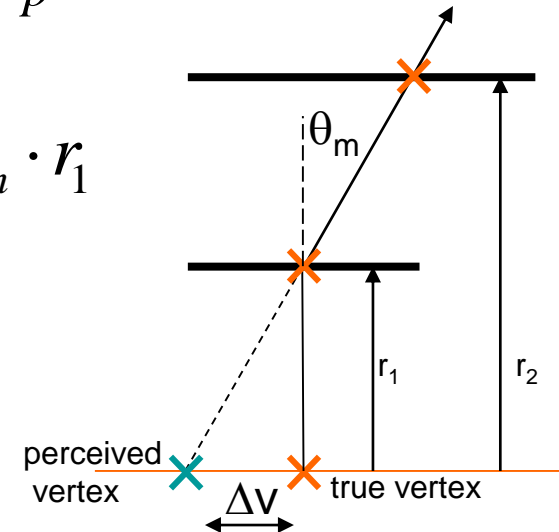
first pixel layer

$$X_0 = 0.3\%$$

more than 3 times
better than anyone
else

$$\theta_m = \frac{13.6\text{Mev}}{\beta \cdot c \cdot p} \cdot \sqrt{X_0}$$

$$\Delta v = \theta_m \cdot r_1$$



$$\Delta x_{\text{vib}} = 5 \mu\text{m} \quad \text{detector vibration}$$

$$\Delta x_{\text{cell}} = \frac{20 \mu\text{m}}{\sqrt{12}} = 5.8 \cdot \mu\text{m} \quad \text{from pixel size, may be better using centroids}$$

$$\Delta x = \sqrt{\left(\frac{20 \mu\text{m}}{\sqrt{12}}\right)^2 + (5 \mu\text{m})^2} = 7.6 \cdot \mu\text{m}$$

$$\Delta x \cdot \frac{\sqrt{r_1^2 + r_2^2}}{\sqrt{(r_2 - r_1)^2}} = 12.4 \cdot \mu\text{m}$$

first term

$$\theta d \cdot r_1 = 24 \cdot \mu\text{m} \quad \text{detector only}$$

$$\theta_{\text{bp}} \cdot r_{\text{bp}} = 12.5 \cdot \mu\text{m} \quad \text{beam pipe} \quad \text{second term}$$

$$\sqrt{(\theta d \cdot r_1)^2 + (\theta_{\text{bp}} \cdot r_{\text{bp}})^2} = 27 \cdot \mu\text{m}$$

total second term